

**PREDICTION TECHNIQUE ON THE EFFECT OF HUMAN
MOTION ON INDOOR RADIO WAVE PROPAGATION**

MD. JAKIRUL ISLAM

**DISSERTATION SUBMITTED IN FULFILMENT OF THE
REQUIREMENTS FOR THE DEGREE OF MASTER OF
ENGINEERING SCIENCE**

**FACULTY OF ENGINEERING
UNIVERSITY OF MALAYA
KUALA LUMPUR**

2013

ABSTRAK

Kegunaan jalur milimeter amat berkembang dalam sistem komunikasi tanpa wayar dalaman oleh kerana ciri-cirinya yang menarik. Disebabkan jarak antara pemancar dan penerima adalah lebih pendek dalam persekitaran yang tertutup daripada persekitaran luar, laluan perambatan gelombang radio frekuensi jalur milimeter amat dipengaruhi oleh bahan-bahan binaan serta pergerakan objek (manusia). Pengesanan sinaran adalah satu kaedah yang digunakan secara meluas untuk meramalkan laluan perambatan untuk mencirikan gelombang radio bagi perancangan dan penubuhan jenis rangkaian tanpa wayar. Bagi melakukan ini, ia memerlukan maklumat yang sangat tepat tentang objek persekitaran realistik. Selain itu, pengiraan sinaran laluan di dalam persekitaran yang dinamik boleh dianggarkan pengiraan yang mahal kerana bilangan besar sinar yang perlu dikesan dalam tempoh yang singkat. Oleh itu, sinar kaedah yang tepat dan cekap yang dapat mengesan telah dicadangkan di sini, adalah berdasarkan pemisahan permukaan, objek pengedaran alamat dan permukaan teknik lompatan. Pendekatan yang dicadangkan menganggap kesan pergerakan badan manusia bagi menyediakan anggaran yang realistic untuk perambatan gelombang. Oleh itu, satu model badan manusia yang dianggarkan telah dicadangkan untuk mensimulasi aktiviti-aktiviti manusia, manakala tiga dimensi (3-D) kiub atau kuboid digunakan untuk objek yang tinggal di dalam persekitaran simulasi. Struktur data Pokok Merah-Hitam menyediakan mekanisme semula objek yang cepat manakala alamat objek teknik pengedaran menghalang objek yang tidak diperlukan untuk mengambil bahagian di dalam ujian persimpangan, sekali gus mempercepatkan pengesanan sinaran. Sebaliknya, pemisahan permukaan adalah satu teknik baru yang boleh membuat kerja bagi mencari sinar laluan dengan mudah dan tepat, kebanyakannya untuk persekitaran 3-D yang kompleks. Di samping itu, pengiraan sinar laluan tepat yang sampai ke penerima selepas pelbagai pantulan,

pembiasaan dan atau pembelauan juga dianggap di dalam disertasi ini. Bagi membuktikan keunggulan dan kerumitan analisis dan perbandingan yang terperinci (berdasarkan sinar ramalan, masa pengiraan dan kuasa yang diterima) antara kaedah yang dicadangkan dan sedia ada yang dibentangkan di dalam kertas ini. Adalah diperhatikan daripada keputusan, kaedah yang dicadangkan meramalkan jumlah yang lebih tinggi daripada sinar dan ia adalah kira-kira 4% dan 16% dan kaedah yang dicadangkan ialah 69.30% dan 91.47% lebih cepat daripada kaedah yang sedia ada, apabila simulasi telah dijalankan di dalam persekitaran yang mudah dan kompleks . Selain itu, kaedah yang dicadangkan dapat menentukan masa yang berterusan selama dua persekitaran yang berbeza dan masa simulasi yang tidak mengikut bilangan objek persekitaran yang tertutup. Keputusan yang diperolehi dapat menarik minat yang besar untuk mengesan kaedah sinar cadangan yang melibatkan pergerakan manusia di dalam persekitaran dalaman yang mudah dan kompleks.

ABSTRACT

Due to the attractive features of millimeter band, its uses are greatly expanding in the indoor wireless communication systems. As the distance between the transmitter and receiver is much shorter in indoor environments than that of the outdoor environment, the radio wave paths of the millimeter band frequencies are highly influenced by the building materials as well as by the human movements. Ray tracing is widely used method to characterize the radio wave propagation for the planning and establishment of the indoor wireless network. Accurate object modeling for the realistic environment and computational time are two classical problems of the ray tracing model. Because, large number of rays that travels in a complex and convoluted indoor environment must be traced. Therefore, an accurate and efficient ray tracing method is proposed here, which is based on the surface separation, object address distribution and surface skipping techniques. The proposed approach considers the effects of human body movement to provide a realistic estimation of the wave propagation. Hence, an approximated human body model is proposed to simulate the activities of humans, whereas three dimensional (3-D) cube or cuboids are used for the remaining objects of the simulation environment. The Red-Black tree data structure provides a faster object retrieval mechanism while object address distribution technique prevents the unnecessary objects to take part in intersection tests, thus accelerates the ray tracing. Conversely, the surface separation is a novel technique that makes the tracing of the ray paths easily and accurately, mostly for the complex 3-D environment. In addition, the calculation of exact ray paths that reach the receiver after multiple reflections, refractions and/or diffractions is also considered in this study. To prove the superiority, complexity analysis and detail comparisons (based on predicted rays, computational time and received power) between the proposed and existing methods are presented in

this study. It is observed from the results that the proposed method predicts the same amount of rays and received power as the image and Space Volumetric Partitioning (SVP) methods, which ensures the accuracy of the proposed method. Conversely, the proposed method predicts the higher amount of rays (it is about 10% and 2%) and higher amount of received power (it is about 3.65% and 1.87%) compared to the Ray Launching (RL) and Angular Z-Buffer (AZB) methods, respectively. Moreover, the proposed method is 30.75%, 36.47, 69.30%, and 91.47% faster than the SVP, AZB, Image, and RL methods, respectively, when the simulation was carried out in the simple and complex environment, respectively. Additionally, the proposed method relatively obtaining the constant time for two different environments and the simulation time does not directly follow the number of objects of the indoor environment. The results obtained will be of great interest for the proposed ray tracing method that involves human motion within the simple and complex indoor environments.

UNIVERSITI MALAYA

ORIGINAL LITERARY WORK DECLARATION

Name of Candidate: **Md. Jakirul Islam** (Passport No: **C0161413**)

Registration/Matric No: **KGA110013**

Name of Degree: **Master of Engineering Science**

Title of Dissertation: **Prediction Technique on the Effect of Human Motion on Indoor Radio Wave Propagation**

Field of Study: **Radio Wave Propagation**

I do solemnly and sincerely declare that:

- (1) I am the sole author/writer of this work;
- (2) This work is original;
- (3) Any use of any work in which copyright exists was done by way of fair dealing and for permitted purposes and any excerpt or extract form, or reference to or reproduction of any copyright work has been disclosed expressly and sufficiently and the title of the work and its authorship have been acknowledged in this work;
- (4) I do not have any actual knowledge nor ought I reasonably to know that the making of this work constitutes an infringement of any copyright work;
- (5) I hereby assign all and every rights in the copyright to this work to the University of Malaya (UM), who henceforth shall be owner of the copyright in this and that any reproduction or use in any form or by any means whatsoever is prohibited without the written consent of UM having been first had and obtained;
- (6) I am fully aware that if in the course of making this work I have infringed any copyright whether intentionally or otherwise, I may be subject to legal action or any other action as may be determined by UM;

Candidate's Signature

Date:

Subscribed and solemnly declared before,

Witness's Signature

Date:

Name:

Designation:

ACKNOWLEDGEMENTS

I would like to express my deepest gratitude towards my supervisor and project leader, Dr. Ahmed Wasif Reza for his invaluable guidance and support throughout my M.Eng.Sc. work. This work would not have been possible without the encouragement and motivation that he provided along with his immense technical expertise. I have learnt a lot from him and it has been honored to work with him. I would also like to thank Dr. Kamarul Ariffin Noordin for his cooperation during my research.

My sincere thanks also go to the University of Malaya for offering me extensive financial support under the University of Malaya Research Grant (UMRG) scheme. Without this financial support, my ambition to study abroad can hardly be realized.

I would like to thank my family and friends whose unconditional love and support has carried me through the tougher times. I must thank my wife for her support and endless patience during the last six months.

Finally, I would like to express my love and gratitude to my parents to inspire me throughout my life.

Last but not the least; I would like to thank almighty Allah who gave me strength and made me capable for the successful end of the research.

TABLE OF CONTENTS

ABSTRAK	ii
ABSTRACT	iv
ORIGINAL LITERARY WORK DECLARATION	vi
ACKNOWLEDGEMENTS	vii
TABLE OF CONTENTS	viii
LIST OF FIGURES	x
LIST OF TABLES	xii
CHAPTER 1: INTRODUCTION	1
1.1 Motivation and Design Challenges	1
1.2 Research Objectives	5
1.3 Dissertation Outline	5
CHAPTER 2: LITERATURE REVIEW	7
2.1 The Millimeter Frequency Band	7
2.2 Why is the 60 GHz Frequency?	8
2.3 Challenges of the 60 GHz Frequency	10
2.4 Measurement Based Propagation Modeling at 60 GHz	10
2.5 Simulation Based Propagation Modeling at 60 GHz	16
2.6 Drawbacks of the Traditional Ray Tracing Algorithms	21
2.7 Summary	27
CHAPTER 3: RESEARCH METHODOLOGY	29
3.1 Object Modeling and Ray Tracing Method	29
3.1.1 Object and Human Body Modeling	29
3.1.2 Object Address Distribution Technique	31
3.1.3 Surface Separation and Calculation of Intersection Point	34

3.1.4	Calculation of the Direction of Ray's	36
3.1.5	Determination of Closest Intersection Point	38
3.2	Ray Tracing Method	41
3.3	Complexity Analysis	47
CHAPTER 4: RESULTS AND DISCUSSION		51
4.1	Performance Evaluation	51
4.2	Effect of Human Movements	55
4.2.1	Effect of Single Human Movements for Different Distance Between Human and Rx	56
4.2.2	Effect of the Multiple Human Movements	58
CHAPTER 5: CONCLUSION		62
5.1	Overall Conclusion	62
5.2	Research Contributions	64
5.3	Future Work	64
REFERENCES		66
LIST OF ISI PUBLICATIONS		75

LIST OF FIGURES

Figure 2.1:	Allocation of electromagnetic frequency spectrum	8
Figure 2.2:	Signal prediction using image method	22
Figure 2.3:	Illustration of the ray launching method	23
Figure 2.4:	Illustration of beam tracing in an indoor environment	26
Figure 3.1:	Walls and partitions are presented by 3-D cube or cuboids	29
Figure 3.2:	(a) approximated 2-D view of a human body (b) simplified 3-D representation of a human body model, which is bounded by 3-D rectangle	30
Figure 3.3:	Illustration of the objects exists on some splitting area	31
Figure 3.4:	Illustrations of object address distribution technique	32
Figure 3.5:	Recursive small rectangle insertion function of the Red-Black tree	33
Figure 3.6:	Illustration of separated surfaces of a 3-D object and intersection point	34
Figure 3.7:	Illustration of (a) reflection and refraction of incident ray within a wall (b) diffraction of incident ray from approximated human body model	37
Figure 3.8:	Closest intersection point (CIP) detection within a single rectangle	38
Figure 3.9:	Closest intersection point detection based on the valid rectangle detection	39
Figure 3.10:	Closest intersection point (CIP) detection within valid rectangles	40
Figure 3.11:	The closest intersection point CI_1 identified based on the distance from the ray's emanating point	41
Figure 3.12:	Illustration of the proposed ray tracing in an indoor environment	42

Figure 3.13: Illustration of ray tracing (a) when movable objects are placed at their initial locations (b) after automatically moved to the new locations	45
Figure 3.14: Proposed recursive ray-tracing algorithm	46
Figure 4.1: (a) Ray prediction and (b) corresponding computation time for the proposed and existing ray tracing methods, which is obtained from two different indoor environments	53
Figure 4.2: Model of LOS blocking by a human body in a complex indoor environment	55
Figure 4.3: (a) Received rays and (b) their computation time variations due to the moving human for different distances between the human and Rx	57
Figure 4.4: (a) Received rays and (b) their computation time variations for the multiple humans are moving parallel or perpendicular to the LOS path	59
Figure 4.5: Comparison based on the received power for different number of humans (a) for six humans (b) for nine humans, when they are moving parallel or perpendicular to the LOS path	61

LIST OF TABLES

Table 3.1: Time complexity of the proposed and existing ray tracing algorithms	50
Table 4.1: Average ray prediction result of the proposed and existing ray tracing algorithms	54
Table 4.2: Specification of the simulation environment	55

University of Malaya

CHAPTER 1

INTRODUCTION

With ever increasing demand of the telecommunications applications, advances in technology and exceptional characteristics of the millimeter (60 GHz) band couple with the large bandwidth available in this unlicensed band have shown a great interest in wireless networks such as Wireless Personal Area Networks (WPAN) and Wireless Local Area Networks (WLAN) because of low cost and high data rate wireless communications. At these frequencies, various losses greatly increase with Transmitter-Receiver separation; which facilitates to reuse frequencies within any particular area, therefore, the network capacity increases significantly. Due to this propriety, interference between the frequency uses reduced dramatically. So that, the establishment of multiple operators by using the high frequency band within the same area is not difficult. Moreover, recent development in Integrated Circuit (IC) design and processing technology has shown potential to make reasonably priced communications systems available as well as the small printed antennas permit cheap packaging of just a few of these ICS into fully functional transmit/receive modules.

In contrast, millimeter (60 GHz) band frequency is highly influenced by the obstacles such as walls and human body due to their short wavelength and high oxygen absorption capacity. Therefore, the knowledge of the basic propagation characteristics at 60 GHz becomes necessary.

1.1 MOTIVATION AND DESIGN CHALLENGES

The indoor wireless network can be characterized by conducting a series of propagation measurements. Based on the measurements, several studies were performed in this frequency band, most of them used simple environment. Most of the time, these

environments were unfurnished or few furnished and consider the human movements within the environment. However, this type of measurements can be very time consuming that provides costlier services for the complex environment. Conversely, propagation models based on the simulation can save time and obtain the similar parameter required to design this kind of networks that will provide a reliable and low-cost service. Therefore, modeling of radio wave propagation prediction has been an attractive research area for many years, and becomes more popular for the high frequency band of interest that shifts with the demands of concurrent communication systems.

Propagation modeling is about determining how a transmitted signal is received after having interacted with a given environment, which fundamentally limits the performance of a wireless system. Propagation occurs in indoor environments via several diverse and complicated mechanisms. Accurate propagation prediction depends on several environmental characteristics such as the electrical properties of the materials present, time variation of the objects as well as the location and orientation of the objects. Moreover, radio wave propagation in the high frequency band (60 GHz) is highly influenced by the movements of objects such as human body and any other objects. Wave propagation in populated indoor environment is dynamic in nature; simple movements of the human body can change entire paths of transmitting waves in the buildings, which may change every parameters of the radio wave propagation.

In order to handle this, some millimeter-wave range channel propagation model (using measurement incorporated with ray tracing) have been found in the literature (Genc et al., 2012; Khafaji et al., 2008; Lim et al., 2007; Xu et al., 2002). The results from the former studies showed that the movement of the human body has significant impact on indoor wave propagation. Among these propagation models, poor human body model, conventional ray tracing algorithms and conventional database are used to characterize

the radio wave propagation for the simple indoor environments. However, to characterize the realistic complex indoor environments, these methods are not suitable in terms of accuracy and computational efficiency. Design challenges of the propagation modeling at 60 GHz frequency will discuss below.

Ray tracing techniques are vastly used in indoor propagation model to predict the radio wave propagations because of the accuracy. In order to provide an accurate simulation results, ray tracing simulations must be performed for a large amount of points, and this leads to unacceptably large computational times. On the other hand, the large building database is needed for the complex indoor environment, which is not easy to implement, and will make the characterization of indoor environments more complicated. Moreover, traditional database is not adequate for the large amount of ray-object intersection test because of enormous database access time. Therefore, the first challenge of the propagation prediction is the successful modeling of wireless network for the realistic indoor environment and this modeling should be based on the efficient and accurate prediction of the radio wave propagation that are transmitted from a fixed transmitter and received by the fixed receivers. In order to accurate prediction of the propagation path of the transmitted signals, the proper modeling of the human body, partition walls and furniture's are extremely important for the indoor environments and this is the second challenge of the propagation model.

The ray tracing model described in (Mohtashami and Shishegar, 2010), it appears that all rays will either be reflected or transmitted through the objects in the indoor environment. However, a true wave propagation model must consider the refraction, diffraction, and penetration of waves along with the reflection of the transmitted waves. Without considering these rays, prediction of ray paths would be inaccurate in an indoor environment. Therefore, a third challenge of the propagation modeling is the accumulation of all propagated waves in the indoor environment. The fourth challenge

of the propagation model is the efficient and accurate building database, for the accurate prediction of the radio wave propagation prediction it also important to ensure that the information about objects that will store in building database are highly accurate and precise. Traditional databases are not enough flexible to modify the information about the propagated waves. Hence, it is desirable to introduce a new data storage method for accurate radio wave propagation prediction, which will overcome these limitations.

Therefore, the main goal of this study is to develop a new ray-tracer and a suitable human body model that is capable of simulating arbitrary populated indoor environments and apply it to study the influence of the human body movements on indoor radio wave propagation. The ray-tracer must be able to compute various parameters at realistic indoor environment at a frequency of 60 GHz. In addition, an approximated human body model is proposed to simulate the activities of humans and remaining objects are created by three dimensional cubes. In order to overcome the limitations of traditional database, many data structures using C sharp object oriented programming were used to store the geometric properties and information about the objects and rays were used in the simulation environment. These data structures work independently in the simulation software, enabling easy to the implementation, and will make the characterization of indoor environments more flexible. This study introduced a number of new algorithms, which obtains better ray prediction results, while the number of ray-object and ray-surface intersections is reduced significantly and thus, greater reduction in simulation time is achieved. For the accurate ray path prediction, surface separation together with the calculation of the accurate direction of reflection, refraction, diffraction, and penetration of propagated waves is considered in the proposed method. Moreover, object address distribution technique and Red-Black tree data structure are used as a new acceleration technique in the proposed method. The

result confirms that the proposed method outperforms compared to the existing methods.

1.2 RESEARCH OBJECTIVES

The objectives of this study are to develop a cost effective, efficient and accurate simulation of the indoor radio wave propagation in presence human motion, which fulfills the following purpose:

- (i) To predicts the effect of human body movement to provide a realistic estimation of the wave propagation.
- (ii) To proposes a suitable human body model and better data (objects and electromagnetic properties) storage system to provide better prediction accuracy.
- (iii) To develop a faster ray tracing approach then apply this algorithm in complex and populated indoor environment to characterize the wave propagation at 60 GHz frequency.
- (iv) To conducts different comparisons between the proposed and existing methods to determine the overall efficiency of the proposed method.

1.3 DISSERTATION OUTLINE

The structures of this dissertation are as follows:

Chapter 1: This chapter provides the introduction to the proposed model, includes background study, objective, problem statement, scope, and proposed methodology.

Chapter 2: Chapter 2 will provide the details literature reviews that are related to the proposed study.

Chapter 3: Proposed methodology and its associated tools are described in this chapter. Reflection, transmission and diffraction mechanisms involved in the ray tracing method are also presented in this chapter. Moreover, detail algorithm and complexity analysis of the proposed method is also provided in this chapter.

Chapter 4: Chapter 4 is about result and discussion. All the analysis of the result will be stated in this chapter.

Chapter 5: In this last chapter, will give the conclusion and also the suggestion for the future work.

University of Malaya

CHAPTER 2

LITERATURE REVIEW

Wireless communication is emerging business and personal communication all over the world. Customers always find comfort to use small communication devices for wireless voice and data communications. The demand for the ever-emerging wireless communications has led to the development of PCS (Personal Communication Systems), WLAN, and WPAN. PCS offers a short-range wireless communication service to a large number of users. It uses low-power transmitters (10-100mW) and the coverage area around 200-400 m in the 1.8-2.2 GHz band. On the other hand, WLAN and WPAN allow networking between fixed and portable computers by using the wireless data link, which utilize 2.4, 3.6, and 5 GHz frequency bands for wireless data communications within a short coverage area. Now a day's, development of multimedia and communication devices (Floyd et al., 2005; Shen et al., 2006) increases user demands for the broadband wireless communication in the homes, offices, and factory buildings. Consequently, advanced multimedia devices like HDTV, IPTV, multimedia game, and VoIP are now available for wireless networks, which require high data rate and high bandwidth wireless communication link. The need for very high data rate couple with huge bandwidth applications (1 Gbit/s or higher) has led to the use of the millimeter band frequency like 60 GHz frequency band in WLAN and WPAN networks.

2.1 THE MILLIMETER FREQUENCY BAND

This day, a wireless network is the essential part of the daily life and its continuous development offers better quality of service and user experience. Millimeter wave technology is one of the rising wireless technologies and has mainly been developed for the military applications. Last few years, progress in technology and low-priced

electronic devices have made the millimeter band as an interesting technology and begun to draw a great interest from educational institutions, industries and other organizations. The millimeter wave technology uses 30-300 GHz electromagnetic spectrum and its wavelength is 10 millimeter to 1 millimeter (Oliver, 1989), as illustrated in Figure 2.1.

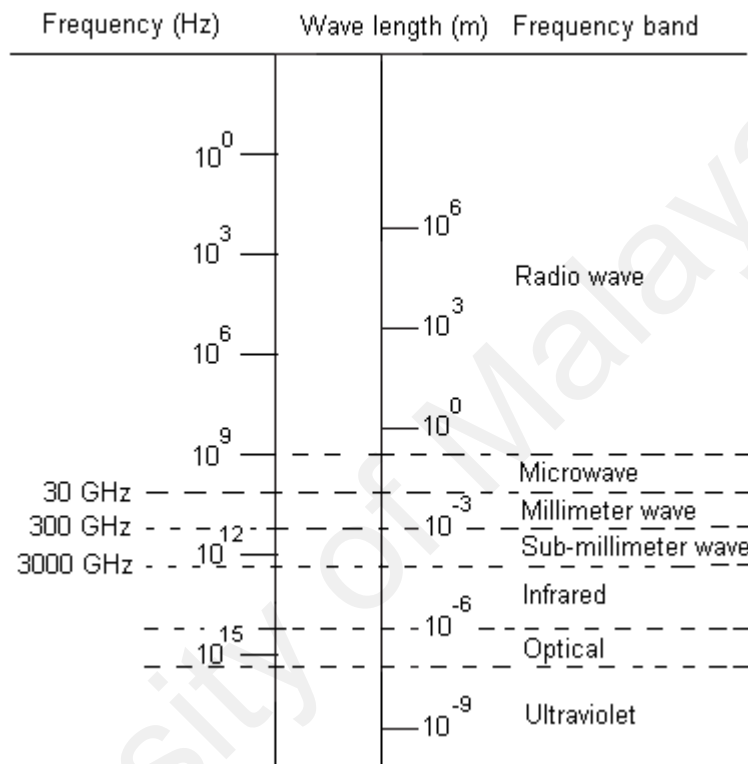


Figure 2.1: Allocation of electromagnetic frequency spectrum.

2.2 CHOICE OF 60 GHz FREQUENCY

The exploding demand for bandwidth has recently confirmed the lack of the traditional microwave frequency allocations. Due to the shortage of unallocated spectrum and the need for interference free channel separation the wireless industry has begun to focus on higher previously unallocated portions of the spectrum. For a number of reasons, the Millimeter wave frequency region from 30 GHz to 300 GHz, is the logical choice available for applying the new standard. The interest in 60 GHz frequency band stems from a phenomenon of nature: the oxygen molecule (O_2) absorbs electromagnetic energy at 60 GHz like a piece of food in a microwave oven. This absorption occurs to a

much higher degree at 60 GHz than at lower frequencies typically used for wireless communications. This absorption attenuates 60 GHz signals over distance, so that signals cannot travel far beyond their intended recipient. For this reason, 60 GHz is an excellent choice for short-range communications. Beside this, one of the major advantages is the huge unlicensed bandwidth. Compare to the unlicensed band used in the ultra-wideband (UWB) system (Qiu et al., 2005; Shen et al., 2006; Win and Scholtz, 2000), the 60 GHz provides 5 GHz continuous bandwidth and it is not limited in terms of power limits. This is because, the UWB band is overlaid system and therefore the mutual interferences experiences worse and worse. The IEEE standards for the UWB are not accepted worldwide and therefore, UWB radio of one region is not useable in another region, but it can be possible for the 60 GHz radio.

The data - rate limitation is another issue for the present UWB systems. The multiband UWB can handle data rates up to 480 MB/s, which is well suited for the compressed video. However, the data rate for the high definition multimedia interface needs 2 Gb/s data rate. Although, multiband UWB can enhanced to support up to 2 Gb/s, but it is concerned with complexity, power consumption and cost. On the other hand, an application that uses 60 GHz frequency can support the transmission at higher power levels and high power levels offer multi-gigabits per second data transfer rate over short distances. Moreover, 60 GHz radio waves cannot penetrate the human body as well as radiation is much lower than the safety limits, therefore, it is not harmful to the human body. In addition, variations in received signal strength are obtained with UWB system, which always makes variations in the coverage area according to the Friis propagation rule. Conversely, relatively less variations in received signal strength is observed in case of a 60 GHz system and thus, coverage range remains almost unchanged on the 60 GHz system. The promising characteristics of 60 GHz frequency promote it as the best candidate technology for gigabit wireless technologies.

2.3 CHALLENGES OF THE 60 GHz FREQUENCY

In spite of the different advantages of the 60 GHz based communications, it experiences a number of vital problems that must be solved. Typically, 60 GHz introduced for the multi-gigabit data rate that operates within the short-range area to support various applications. Within this data rate and range, it is a crucial task for the 60 GHz systems to offer adequate power margins to make sure the consistent communication link. Moreover, electromagnetic waves cannot diffract around the obstacle when the size of the obstacle is larger than the size of the wavelength. But, communication links at 60 GHz are directly affected by obstacles such as walls, furniture as well as human body because of the very small wavelength, which is about 5 millimeter. Previous study shows that blockage by a human can provide 20-30 dB loss. Therefore, human body movements in the indoor environment can cause irregular blockage in communication links, as a result a time-varying network topology is experienced in millimeter-wave propagation. In order to maintain the continuous network connectivity and ensuring the the better quality of service for high-speed data communication in such a situation is a challenge for indoor network design, which is different from that at lower carrier frequencies. To face this challenge, a suitable propagation model is needed, which takes into account reflection, refraction, and diffraction as well as the movement of the objects, both for the design and for performance evaluation of the 60 GHz indoor networks.

2.4 MEASUREMENT BASED PROPAGATION MODELING AT 60 GHz

Proper design and systematic evaluation of the indoor wireless networks requires a realistic propagation model and it is the first step of the deployment of any wireless network. A realistic propagation model can provide detailed parameters of the radio

wave propagation, which facilitates to study the achievable performance of the wireless networks.

The research about propagation modeling at 60 GHz is started from 1980's and it begins by using the statistical model. A statistical model based on the measurements at 60 GHz is presented in (Wales, 1990). In this model, propagation channel viewed as a linear filter and it is modeled by using the concept of tapping delay line, where the parameters of the tapped delay line are the number of taps, the tap delay, and tap gains. The random process describes these parameters. Mathematically, the impulse response of this filter is as follows-

$$h(\tau, t) = \sum_{i=0}^{N(t)-1} h_i(\tau, t) \delta(\tau - \tau_i(t)) \quad (2.1)$$

In this model, channel response is used to investigate the behavior of the radio channel at 60 GHz frequency. The obtained result shows that, a Poisson renewal process could be used to model the time delay sequence. Conversely, lognormal distribution is much better than the anticipated Ricean to fit the measured data for the component amplitudes.

Same authors present a new paper in (Wales et al., 1991). In this paper, they made some modifications on impulse response of linear filter describe in (Wales, 1990) and confirms that the delay spreads is 50 ns exist and received power decreases with increasing delay compared to the lowest operating frequency.

In (Davies et al., 1991), wideband propagation measurements are conducted at 1.7 GHz and 60 GHz. The main goal of this study was to compare the levels of multipath activity at the two frequencies. They used RMS delay spreads to determine the levels of multipath. The result shows that the levels of multipath at two different frequencies are

directly depend on the size of the rooms and the measurement procedure. Moreover, they found a negligible difference in atmospheric absorption at both frequencies.

To review the indoor wave propagation characteristics, another measurement (at 60 GHz) based statistical propagation model is presented (Bensebti et al., 1991). In this paper, multipath channel is modeled by absorptive and dispersive time-varying delay line with L paths, which is a function of time and location. Thus, the channel impulse response for k^{th} path is presented by-

$$h(t) = i(t) + jq(t) = \sum_{k=1}^L a_k \delta(t - \tau_k) \exp(j\theta_k) \quad (2.2)$$

After investigating the behavior of this channel, they found that the narrow band signal is attenuated quickly over short distances and delay spread (10 to 40 ns) depends on site size and the polarization of waves.

A theoretical propagation model based on Geometric Optics (GO) and Fresnel diffraction for corridor scenario is presented in (Hammoudeh and Haslett, 1995). This model determined the signal envelope variations by considering a direct/direct-penetrated ray, diffracted ray and reflected/reflected-penetrated rays up to the third order at 60.4 GHz frequency. The result shows that the predicted envelop is 10 dB below compared to the measured value.

Another propagation model based on measurements (at 17 GHz and 60 GHz) presented in (Nobles and Halsall, 1999). Based on the Friis (Friis, 1946) equation, this paper presented a model for path loss within a room scenario and it is expressed as follows-

$$L_p = 10 \log_{10} \left[\left(\frac{1}{4\pi r^2} + \frac{4}{R} \right) \times \frac{\lambda^2}{4\pi} \right] \quad (2.3)$$

Where, L_p is the path loss at distance d , λ is the wavelength. On the other hand,

$$R = \frac{(1 - \bar{\alpha})}{\sum S\bar{\alpha}} \quad (2.4)$$

Where, S is the total surface area of the room, $\alpha = 1 - \rho$ is the absorption coefficient ratio, and $\bar{\alpha}$ is the average absorption coefficient for the room. After doing this investigation by using this formula, they proposed that 17 GHz band is suitable for High Performance European Radio Local Area Networks (HIPERLAN) and 60 GHz is suitable for the broadband wireless communication system.

In (Delignon et al., 2001), statistical multipath channel impulse model for 60 GHz indoor wireless systems is presented. The author of this paper considered all physical phenomenon's that responsible for the influence of indoor propagation and showed that this model can be suitable for any types of room. This model assumes that rays are arrived at the receiver in cluster mode and Poisson processes is used to model the time of arrival of clusters and the time of arrival of the rays. After measurements, they proposed that Rayleigh model is not suitable for 60 GHz propagation and therefore, this model has shown the coefficients of the channel impulse response are K-distributed and it is expressed as follows-

$$h(t) = \sum_{k=1}^{\infty} h_k(t) \quad (2.5)$$

Where $h_k(t)$ is the k^{th} cluster impulse response and it is expressed as-

$$h_k(t) = \sum_{l=1}^{\infty} h_{k,l}(t) = \sum_{l=1}^{\infty} \beta_{k,l} e^{j(2\pi f_c \tau_{k,l} + \theta_{k,l})} \delta(t - T_k - \tau_{k,l}) \quad (2.6)$$

After some simplification, this impulse response presented as-

$$h(n) = \sum_{K=1}^N h_k(n) \quad (2.7)$$

and $h_k(n)$ represented as-

$$h_k(n) = \sum_{l=1}^{N_k} \beta_{k,l}(n) e^{j(2\pi f_c \tau_{k,l}(n) + \theta_{k,l})} \quad (2.8)$$

where N is the number of cluster and N_k is the number of rays of k^{th} cluster.

In order to investigate wideband propagation characteristics for indoor broadband wireless LAN at 60 GHz frequency, a measurement-based model is proposed in (Siamarou, 2003). The wideband propagation characteristics of the millimeter indoor radio channel are determined from the complex low pass impulse response, power delay profile, and frequency selective behavior and expressed as follows:

The channel impulse response is-

$$h(\tau) = \sum_{n=1} a_n e^{j\theta_n} \delta(\tau - \tau_n) \quad (2.9)$$

where a_n , θ_n , and τ_n are the amplitude, phase, and delay of the ray n , respectively.

The power delay profile is calculated from-

$$p(\tau) = \sum_{n=0} a_n^2 b^2(\tau - \tau_n) \quad (2.10)$$

where, $b(\tau)$ represents base band pulse shape. On the other hand, frequency selective behavior is represented by the following equation-

$$R(\Delta f) \cong \int_{-\infty}^{\infty} H(f) H^*(f + \Delta f) df \quad (2.11)$$

The measurements had been conducted in a single room and corridor scenario. After analysis the complex frequency responses, this study observed that the coherence bandwidth influences significantly with the location of the receiver.

Moreover, to characterize the indoor wideband parameters, measurements have been conducted at 60 GHz and 2 GHz in (Yang et al., 2005). In this paper, Normalized Received Power (NRP) and RMS delay spread is calculated to compare the channel characteristic at these two frequencies. The obtained results show that NRP and RMS delay spread at 60 GHz is much lower than the 2 GHz. Recently, a large-scale fading

model for statistical characterization of indoor radio channels operating in the 60 GHz frequency is introduced in (Smulders, 2009). This study emphasizes on both the large-scale fading and small-scale fading analysis of the office environment. The result shows that, the path - loss exponent for the LOS path is similar compared to the conventional microwave frequencies. In case of small-scale fading, Doppler spread, delay spread and angular spread are considered. From the results of Doppler spread, the authors confirm 60 GHz can support multi-gigabits transmission, which encountered slow fading. Similarly, small variations on the RMS delay spread are found from the investigated results. Moreover, the author proposed various solutions to take care about the different challenges regarding the optimal deployment of the 60 GHz systems.

In order to investigate potential and feasibility of 60 GHz radios for very high data-rate short-range communications in medical applications, measurements have been done in a shielded room to characterize wave propagation in (Kyro et al., 2010). A link budget and delay domain multipath characteristic is studied. From the results of measurements, it can be found that the power index is closed to 4 and path-loss varies up to 6 dB. Beside this, many researches on 60 GHz frequency can be found in (Bird et al., 1994; Chahat et al., 2012; Daniels and Heath, 2007; Garnier et al., 2002; Jacob et al., 2010; Langen et al., 1994; Liihteenmiiki and Karttaavi, 1996; Maltsev et al., 2009; Minyoung and Gopalakrishnan, 2009; Moraitis and Constantinou, 2004; Morgadinho et al., 2012; Siamarou, 2003; Zhong, 2008; Zwick et al., 2005).

As the explosive growth of the wireless communications all over the world, it is a crucial task to have obtained suitable data rates, estimating their coverage, determining the type of antenna and all other parameters by taking into account all effects involved in the 60 GHz wave propagation, without the measurements, which are expensive and time consuming. It is evident that the parameters that influence the indoor radio wave propagation at 60 GHz are very complex and diverse. Therefore, propagation modeling

is still interesting research subject to the researchers. Finally, it is an essential task to develop an effective simulation based propagation models for wireless communication to provide design guideline for wireless systems.

2.5 SIMULATION BASED PROPAGATION MODELING AT 60 GHz

Wave propagation in indoor is different from the outdoor one. Likewise, modeling of indoor wave propagation is different from outdoor propagation modeling as well because of large changeability in building layout and materials used. Additionally, the simple movement of people, furniture, doors, appears frequent change in the environment and so on. Resulting, the propagated radio waves reached the receiver by simple line-of-sight propagation and/or multiple reflections, refractions, diffractions or transmission and these are dynamically change with the environment, which makes the propagation modeling more complicated and interesting as a research subject. In general, two types of propagation model can found in literature namely (i) deterministic (ii) stochastic modeling. Deterministic approach is wide used technique to model the wave propagation for the indoor environment and it can be divided into two sub-categories, namely- (a) empirical (based on measurements) (b) ray tracing approach.

The empirical approach takes out the propagation parameters from the measurement data, which are accumulated from a specific environment. Empirical models are easier to implement, spends less time to compute the propagation paths as well as less sensitive to the environment's geometry and therefore obtain less accuracy. Moreover, it is critical for these types of models to collect sufficient information about the interesting environment. Additionally, this type of models becomes even more expensive if any change in the environment has happened, for example by relocating the mobile station or reorganization of furniture in the environment as well as human movements. Such changes need a recalibration of the propagation model mandatory. Many propagation

models based on empirical approach for 60 GHz have been developed and reported in the literature (Anderson and Rappaport, 2004; Hansen, 2002; Janaswamy, 2006; Lostalen et al., 2002; Moraitis and Constantinou, 2002; Smulders and Correia, 1997).

Ray tracing is widely used in deterministic approach, which used advanced electromagnetic theory, Geometrical Optics (GO) and Uniform Theory of Diffraction (UTD) to simulate the wave propagation (Kouyoumjian and Pathak, 1974). In this approach, location, size and orientation of the receiver (Rx), transmitter (Tx) and different types of objects are positioned in the environment according to the real arrangement. Then, the signal is transmitted from the Tx in different directions. Once the receiver receives the signal, propagation parameters are calculated in order to characterize the propagation mechanism. A number of ray tracing models for 60 GHz systems have been presented in (Algiannakis et al., 1995; Dardari et al., 1996; Degli-Esposti et al., 1997; Diskin and Brennan, 2007; Fernandes et al., 1994; Fluerasu and Letrou, 2009; Gustafson and Tufvesson, 2012; Haibing et al., 2006; Jacob et al., 2013; Jarvelainen et al., 2012; Khafaji, 2008; Lim et al., 2007; Lostalen et al., 2002; Rougeron et al., 2002; Sandor et al., 1997; Tam and Tran, 1995; Williamson et al., 1997; Yongming et al., 2006; Young-Keun et al., 2011; Youssef et al., 1994). Details of these models are described in the following paragraphs.

In (Youssef et al., 1994), image based ray tracing method is used to model the indoor propagation. They calculated the attenuation and delay spread by performed the simulation within the L - shaped building. The results show that the delay spread is directly decreasing with the distance between transmitter and receiver while attenuation remains low within the less (typically -63 dB) obstructed regions but the normalized received power falls below -100 dB in case of obstructed regions. On the other hand, the model described in (Williamson et al., 1997) is used image based ray tracing method to study the characteristic of the wave propagation in indoor and the simulation result is

used to study the performance of different antennas at 60 GHz frequency. This paper proposed that the switched-beam directional antennas is suitable for reducing the multipath effects of a 60 GHz system. Similarly, (Haibing et al., 2006) developed an image based 3-D ray tracer to characterize wave propagation in the single room scenario. This paper conducted various analyses such as channel fading, multipath waves mapping into delay and angular domain, and multipath dispersion with respect to the time and space for design of suitable smart antenna. In order to characterize the indoor wave propagation at 60 GHz, another image based 2-D ray-tracing model is presented in (Dardari et al., 1996; Haibing et al., 2006; Williamson et al., 1997). This model calculates the large-scale received power, Rice factor, delay spread as a function of distance as well as small-scale variations in the presence and absence of furniture's. After investigation, they proposed a two-model for the indoor wave propagation. A propagation prediction model based on geometrical optics is presented in (Fernandes et al., 1994). This model analyzed the influence of objects on radio wave propagation inside the small and medium size rooms by ray tracing simulation. In (Khafaji, 2008), image based ray tracing model is used to study the influence of human movement within the single room scenario at millimeter band frequency. In order to investigate the influence of human movement, this paper used a parallelepiped circumscribed with SALT cylinder model for simulating the activity of the human body. RMS delay spread, level crossing rate (LCR), and magnitude behaviors is deeply investigated in this paper. The temporal channel variations or fading effects become fast with respect to the number of people increases is reported in this paper.

Ray Launching (RL) based propagation model is reported in (Lostanlen et al., 2002) for WLAN at 60 GHz frequency of the static indoor environment. This model analyzed both the LOS and NLOS behavior of the wave propagation inside the building. Finally, a simulated data are compared with the measurement data, which shows better

agreement with each other. Likewise, a human blockage model for the IEEE 802.11ad at 60 GHz propagation channel model is investigated in (Jacob et al., 2011). This paper investigates the influence of human movement on 60 GHz channel. Therefore, ray tracing based on RL method coupled with the electromagnetic diffraction model and a random walk model is used in this research. All simulations have done in a conference room scenario and found that knife-edge diffraction model is suitable for the human blockage at 60 GHz frequency. This paper used a multiple knife-edge model instead of double knife-edge model for the prediction of human activity. Moreover, it can be observed from the result that power attenuation is around 50 dB in usual cases but a little bit higher in some cases, which about 60-70 dB. Additionally, the influence of human movement on the small-scale channel parameter is also investigated, and the result shows that the RMS delay spread is increased with the presence of human blockade.

Shooting and Bouncing Ray (SBR) based 3-D ray tracing is proposed in (Lim et al., 2006), they extract propagation parameters such as mean excess delay and RMS delay spread from static indoor environments. The results of the fading analysis were shown to obey a Weibull distribution, which is helpful to predict the channel capacity limit to deploy a high-speed radio link.

A 3-D beam lanching propagation algorithm is introduced in (Fluerasu and Letrou, 2009) to propagation modeling at 60 GHz for the simple environment. Simulations have been carried out in indoor environments. They extracted amplitude delay profile, mean excess delay, and RMS delay spread and compared with the measured and published data to validate the model.

Roughness of the object surface has also impact on radio wave propagation. Therefore, propagation modeling based on Kirchhoff approximation and ray tracing is presented in

(Young-Keun et al., 2011). The ray tracing method called PDM (Alvar et al., 2008) is used in this paper. This paper determined the propagation characteristic due to the roughness of the object surface at millimeter wave. The result shows that roughness at millimeter wave causes deep fading. Many others researches based on the image and RL ray tracing methods to characterize 60 GHz radio channel can be found in (Collonge et al., 2004; Genc et al., 2012; Jacob et al., 2013 ; Marinier et al., 1998; Rao et al., 2011; Talbi, 2001).

Among these models, following drawbacks have been found, which are listed below-

- (i) Simulation conducted in two dimensional (2-D) site-specific static indoor environments, which provides less simulation accuracy than the three dimensional (3-D) indoor environment.
- (ii) Simulation performed in either single room or conference room scenario, but wave propagation characterization in multiple room scenarios is still under investigation.
- (iii) Some of them are considered the dynamic simulation environment where furniture and human body movement is taking into account. Among these models, poor human body model is used, which might not be suitable for the accurate simulation of human activity.
- (iv) For the site-specific model, conventional database is used to store the site-specific simulated object, which is not suitable for the dynamic environment because of the database access delay.
- (v) Finally, these models are used traditional ray tracing method to predict the wave propagation in indoor scenario at 60 GHz frequency.

As the main goal of this research is to develop an efficient and accurate ray tracing model. Therefore, basic operation and disadvantages of the traditional ray tracing methods that are mentioned earlier will describe in the next section.

2.6 DRAWBACKS OF THE TRADITIONAL RAY TRACING ALGORITHMS

In deterministic propagation models, ray tracing is used to determine the propagation paths of the transmitted signals. After identifying all possible paths, high frequency electromagnetic techniques in (Burnside and Burgener, 1983; Kouyoumjian and Pathak, 1974; Luebbers, 1984) are applied to evaluate each signal. In general, the most time consuming operation in a ray tracing method is the ray-surface intersection test. This test is performed each time for every new ray segment generated in the simulation process. When the number of objects involved is relatively large, the ray tracing operation would be very slow. Thus, the computation time is the biggest issue against the development of the ray-tracing methods.

To solve this issue, many ray tracing techniques based on the 2-D method is found in the literature. 2-D models are faster but less accurate compared to the three dimensional method. Because, the 2-D models only traces the fewer rays that are propagated through the horizontal direction. On the other hand, 3-D models are slower but provide better ray prediction accuracy, because it can trace all the rays that are propagated in any direction. In order to overcome the drawbacks of the 2-D model, huge 3-D ray tracing methods already been developed. Most of them are based on Image method, Brute-Force (BF) method (Dersch and Zollinger, 1994), Ray Launching (RL) method, Shooting-and-Bouncing-Ray (SBR) method, and Angular Z-Buffer (AZB) (de Adana et al., 2000; Saeidi and Hodjatkashani, 2010) methods.

The basic idea of image method is proposed by McKown and Hamilton (McKown and Hamilton, 1991) and predicted in Figure 2.2. The main advantage of the image source

method is its robustness. It can predict all the specular paths up to a given order will be found, which ensures the accurateness of the image method. Conversely, the image method suffers from inefficiency. When the number of objects involved is large and there are many reflections for a single path from transmitter to receiver, this method suffers from large computation time. Its computation complexity has exponential growth. In general, $O(S^r)$ virtual sources are generated for r reflections with S surface planes in the environments. The image method is suitable for the simple environments having few objects. However, many indoor environments with which we are concerned in our daily life are furnished and complex. The image method is not adequate to analyze those environments. Therefore, the application of the image method is very limited to indoor radio propagation prediction.

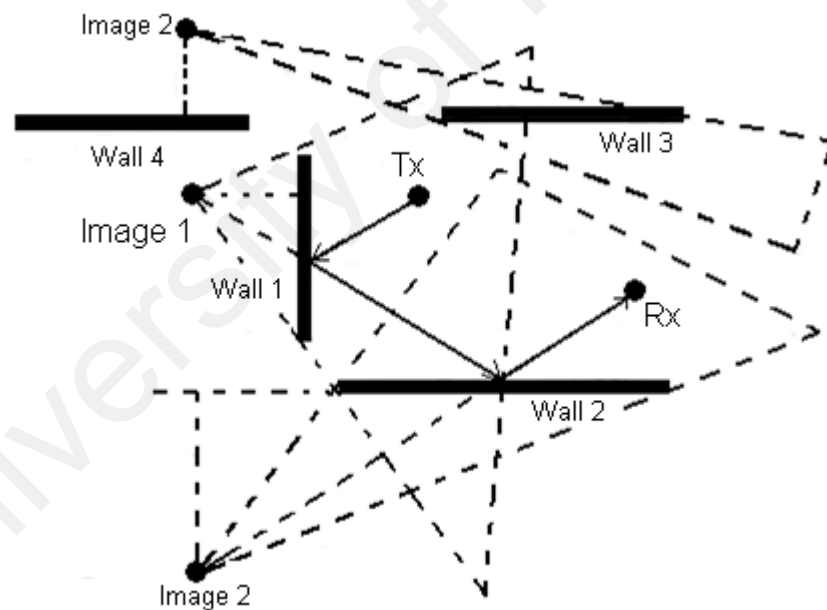


Figure 2.2: Signal prediction using image method.

Brute-Force (BF) (Dersch and Zollinger, 1994; Saeidi et al., 2006) method launches rays in all feasible directions and obtains better accuracy. However, the main disadvantage of BF method is an increasing ray prediction time that grows

geometrically with the analysis area, complexity of the environment, the number of considered effects, or the number of rays launched and tested.

Ray launching is a ray-path searching algorithm as reported in (Hoppe et al., 1999), (Raida, 2008), (Lawton and McGeehan, 1994), and (Sato and Shirai, 2008), (Sato and Shirai, 2009). The ray-launching algorithm launches rays in discrete angle increments from the transmitter and determines their path through a building. If there is an intersection between a ray and an object, the specular reflection angle is computed and the penetrated and reflected rays are launching independently from each other. If the ray passes an edge, all rays on a diffraction cone (Ramo, 1997) must be considered. Therefore, an angle increment is defined and a discrete number of rays are launched from the diffraction point. To ensure the accuracy, the number of rays must be large enough to adequately characterize the multipath propagation conditions. Moreover, a small constant angular separation between launches rays must be specified to produce reliable results. Moreover, the accuracy of ray launching is greatly reduced for those rays traveling long distances from the transmitter (divergence). In these situations, such ray tracers may miss important interactions and thus, it can be said that, ray-launching technique is suffering from accuracy in terms of signal prediction. The concept of ray launching is illustrated in Figure 2.3.

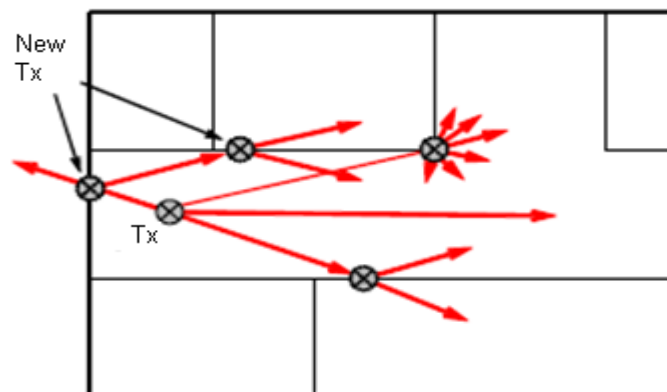


Figure 2.3: Illustration of the ray launching method.

The shooting and bouncing algorithm (Dikmen et al., 2010; Liang et al., 2008; Mohtashami and Shishegar, 2010; Mohtashami and Shishegar, 2010; Mohtashami and Shishegar, 2012; Saeidi et al., 2009; Tao et al., 2008; Wang et al., 2008) launched the rays with a predefined angular separation from the origin of the transmitter. The purpose is to make ensure that none of the wall faces are missing at large distance from the receiver, and all paths are traced until a given power threshold is reached (Kim et al., 2009). In brief, after launching a ray from the transmitter, SBR method checks the condition of the intersection that is the ray intersect with wall surface or an edge. If the ray hits the surface, a reflection is produced and diffraction is produced if the ray hits the edge. Finally, if the ray intersects with the receiver, then the ray tracing procedure stops and calculates the ray characteristics. This procedure is repeated until a certain number of rays are reached. In SBR technique, ray tubes are used to cover the spherical wavefront at the receiving location. If a receiver (R_x) is located in the overlapping area between the ray tubes, the R_x will then receive two rays and hence, ray double counting error will be occurred. In addition, the intersections between the rays and objects are a classical problem in computational geometry and graphics (O'Rourke, 1993). The SBR algorithm tests all the objects to determine whether a ray intersects with an object. If the number of objects are large in the indoor environment, the intersection test can be very time consuming and inefficient. It is noticed in (Catedra et al., 1998) that the intersection test can take more than 90% of CPU time for a general SBR algorithm. To overcome these disadvantages and accelerate the ray tracing, modified wavefront decomposition (MWD) method is introduced in (Mohtashami and Shishegar, 2012). In MWD, binary space partitioning (BSP) technique is used for the acceleration of the ray tracing method. However, a BSP tree with S number of facet needs $O(S)$ time for the worst case condition and $O(S \log S)$ time for the best case condition while performs an intersection test, which are still big enough.

Another ray tracing based on angular Z-Buffer algorithm is presented in (de Adana et al., 2000; Saeidi and Hodjatkashani, 2010). According to this algorithm, the simulation space is divided into a number of angular regions and stores each facet of the environment in the regions array where they belong. Afterward, for each ray, only the objects of a particular region take part in ray-facets intersection tests. From this discussion; it is needed to distribute the S number of facets among the circular regions and its waste $O(S)$ time. After that, a search operation is made to identify the particular region among the X regions, which will spend another $O(X)$ time. Therefore, $O(SX)$ time is needed prior to the intersection time. Whereas, $O(S')$ is needed for a single intersection test, where S' is the number of facets exist in a particular angular region. Moreover, this method not suitable for multiple reflections, because there are many source points and an AZB is needed to build for each of them (Iskander and Yun, 2002). From above discussions we may conclude that, an efficient ray-tracing algorithm is desirable to improve the performance and the accuracy of signal prediction since more complex types of propagation environments are needed to be taken into account.

Prior Distance Measures (PDM) method (Alvar et al., 2008), the number of ray-surface intersection tests are reduced by distance measures between surfaces that is stored in the two $m*n$ dimensional matrices. It is obvious that this method shows a better performance in a simple environment. However, this method fails to reduce the simulation time in case of complex environments. Because, the information retrieval time of these two matrices is also $O(mn)$.

The beam lanching algorithm is introduced in (Fluerasu and Letrou, 2009; Ghannoum et al., 2009; Letrou, 2007; Tahri et al., 2002). The working procedure of the beam launching algorithm is as follows:

- (i) Launch a beam in a certain direction.
- (ii) If this beam intersects with a surface than reflected and transmitted beams are created, which are used as incident beams for the next interaction with a plane.
- (iii) A file is created so that every geometrical characteristic are stored into this file.
- (iv) Finally, follow the same procedure for every beam.

An example of beam tracing in an indoor environment is predicted in Figure 2.4. In case of simple environment, Gaussian beam launching algorithm is faster than any traditional ray-tracing algorithm. However, it is quite hard to implement for the complex indoor environment because of complex mathematical equations need to follow for each Gaussian beam.

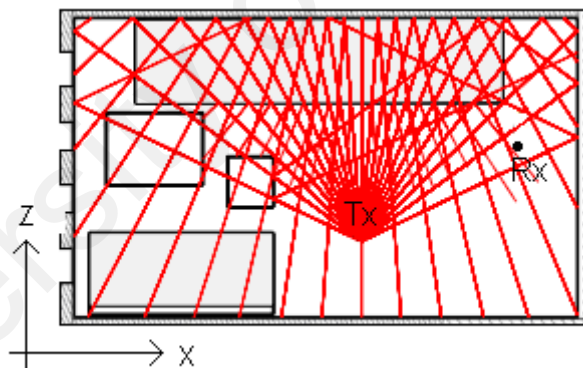


Figure 2.4: Illustration of beam tracing in an indoor environment.

The above ray tracing algorithms is used to predict the site-specific radio propagation characteristics, in spite of its computational intensity. A naive implementation of these models can be computationally expensive. In a large building, there may be many possible propagation paths between transmitter and receivers, due to the convoluted environment and human movements. The above discussed ray tracing algorithms are not

adequate about identifying the signals propagate in the presence of the human movements.

2.7 SUMMARY

Ongoing researches show that the millimeter band is suitable for the short range high speed wireless data communications and therefore indoor networks are the first target of the millimeter band frequency wireless communications. One of the vital factors, which may influence the use of the millimeter - wave technology in indoor networks, is the communication reliability. Therefore, it is a crucial task to characterize the indoor radio wave propagation at a millimeter band frequency to ensure satisfactory performance of an indoor wireless communication system. Therefore, measurement based many researchers for 60 GHz frequency have been reported in literature. Since, measurement based models are costly; simulation based models have been developed as a suitable low-cost alternative. Two major types of propagation models have been found in literature namely empirical and deterministic propagation models to characterize the wave propagation at 60 GHz frequency. Empirical models are based on measurement data, which is costly and time consuming. Moreover, the accuracy of the empirical models is highly depending on the measured data. The main disadvantage of the empirical models is that the model for the one environment cannot be used for another environment without modifications. On the other hand, deterministic models are based on numerical methods such as the ray-tracing method (Liang and Bertoni, 1998; Seidel and Rappaport, 1994) and the finite-difference time-domain (FDTD) method. The main drawbacks of the deterministic approach are the large computational time because of excessive ray-object intersection tests and large database access time for the retrieving the objects or update the information of electromagnetic properties of the rays. Moreover, the accuracy of the deterministic models is highly environment-specific and it highly depends on the shape and orientation of the objects, materials used in the

environment as well as the frequency used for the communication channel. Based on deterministic approach, few propagation models at 60 GHz frequency can be found in literature that already mentioned earlier. They performed the simulation within a room or corridor scenario by using the traditional ray-tracing algorithm. The simulation environment is seemed to be 2-D static environment, where every object remains fixed during the simulation. Few of them are handled with dynamic environment where a poor human model is used to simulate the activity of human movement within the indoor environment. Moreover, these models use traditional database to store the environment objects. Therefore, these models fail to provide sufficient accurate simulation result as well as the simulation time for the realistic simulation. Now it is a big challenge to search for a new accurate and efficient propagation model and design tool that will avoid the disadvantages of the existing models.

CHAPTER 3

RESEARCH METHODOLOGY

In this dissertation, a new human body model along with an accelerated and accurate algorithm is presented for the modeling of the real life indoor radio wave propagation. The proposed ray tracing technique is developed to offer successful predictions of radio signals in the presence of human movements. And the presented human body model is used to simulate the human activity in the indoor environments.

3.1 OBJECT MODELING AND RAY TRACING METHOD

Ray tracing (Aparicio et al., 2011; Reza et al., 2012) is vastly used in radio wave propagation prediction. One of the problems of ray tracing is the computational burden because of excessive ray-object intersection test. Hence, with the intension of reduction of ray prediction time, a new 3-D ray tracing for the complex indoor environment (including human motion) is explored in this study. Before describing the proposed method, some essential tools have been described below.

3.1.1 OBJECT AND HUMAN BODY MODELING

The objects of the simulation environment (walls, partitions, and furniture) have constructed by 3-D cubes or cuboids, which is shown in Figure 3.1.

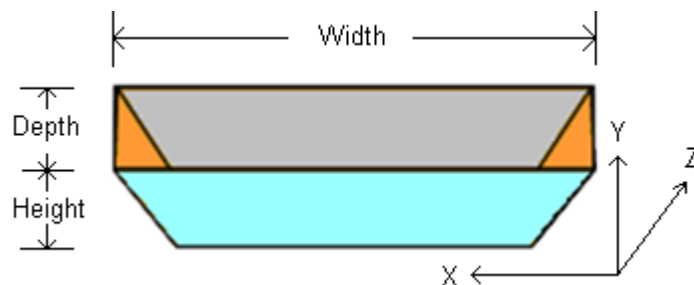


Figure 3.1: Walls and partitions are presented by 3-D cube or cuboids.

An approximation of the 2-D human body is illustrated in Figure 3.2(a), where head, hand and body are represented by the 2-D rectangles. Conversely, a 3-D version of the proposed human body model is projected in Figure 3.2(b). Here, we have used a 3-D rectangle limit to simplify the proposed body model. Khafaji, A. *et al.* (Khafaji, 2008) has presented a human body model whose height of the rectangle limit is 1.70 m, whereas both width and depth is 0.305 m. It can be observed that the width and depth of the human body are not equal in size; therefore, this study used the average height, width, and depth of the rectangle limit of the proposed human body model is 1.70 m, 0.56 m, and 0.305 m, respectively.

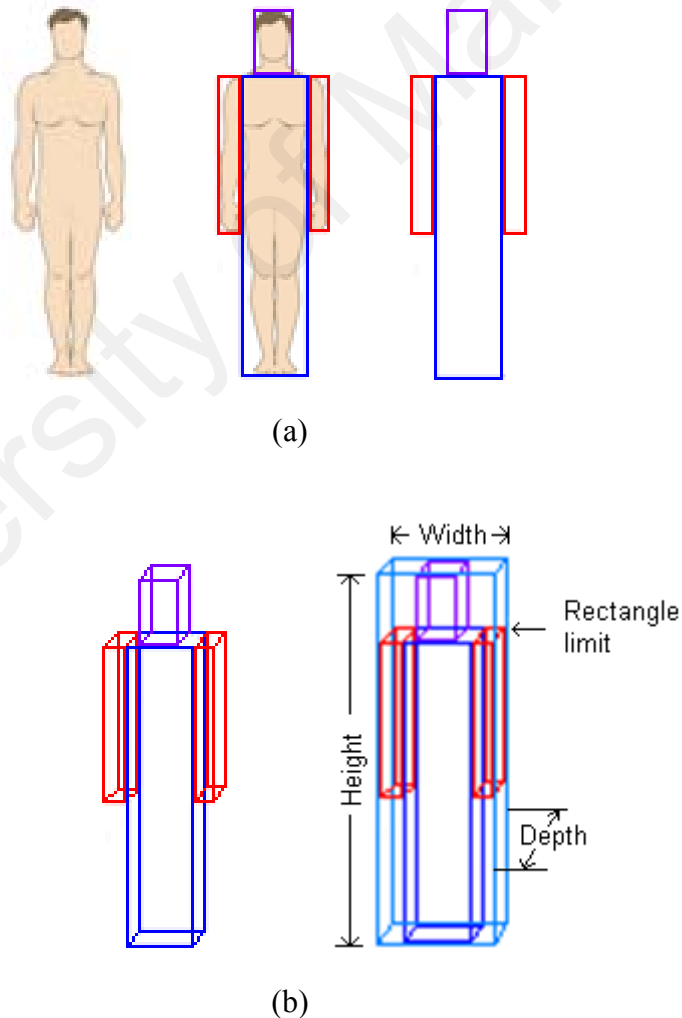


Figure 3.2: (a) approximated 2-D view of a human body (b) simplified 3-D representation of a human body model, which is bounded by 3-D rectangle.

3.1.2 OBJECT ADDRESS DISTRIBUTION TECHNIQUE

In ray tracing models, extensive search of ray-object intersections is needed to accomplish the ray tracing in 3-D planner spaces and thus huge amount of computation time is spend here. To reduce the intersection time, object address distribution technique coupled with the Red-Black tree data structure is presented in this section. In this study, the object addresses are distributed according to the space splitting technique (a technique that splits the entire simulation space to a given number of small rectangles, as illustrated in Figure 3.3). For the simple indoor environment, the number of small rectangles should not exceed 4 and it should be 9 to 16 for the complex indoor environments.

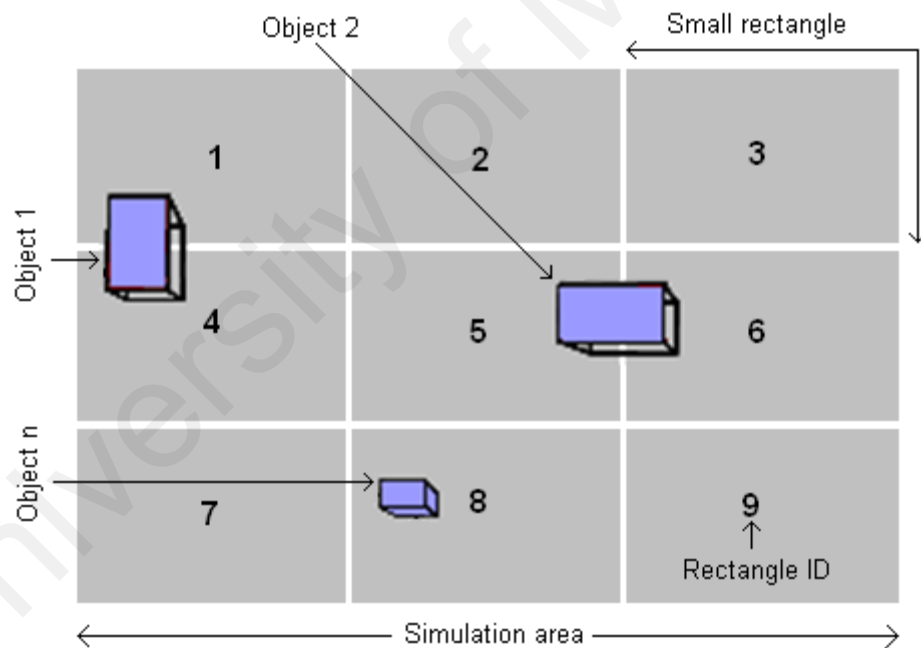


Figure 3.3: Illustration of the objects exists on some splitting area.

After splitting the simulation area, the information of newly formed rectangles has to store in the Red-Black tree nodes as shown in Figure 3.4. Later on, at the time of object creation in the simulation space, each object is to be stored first in an object list (shown at the bottom side of Figure 3.3). Then, the corresponding address of these objects will

be stored in the pointers of the desired tree nodes, namely, object address distribution technique. For instance, referring to Figure 3.3, object 1 exists on the rectangles 1 and 4; if object 1 is stored in an object list at position 1 then the address of this object is needed to store in the tree nodes 1 and 4, as shown in Figure 3.4. Similarly, object 2 exists on the rectangles 5 and 6 and if it is stored in an object list at position 2, then this address will be stored in nodes 5 and 6 of a Red-Black tree (creation of the Red-Black tree according to the proposed method is given in Figure 3.5). This study selects Red-Black tree for storing the splitting part of the simulation area and corresponding object addresses. Because, the worst case computational complexity of the object retrieval operation of a Red-Black tree is $O(\log_2 N)$ (Thomas et al., 2001), where N is the number of split parts (small rectangles) of the simulation environment. However, an object list having N split parts needed $O(N)$ time in the worst case.

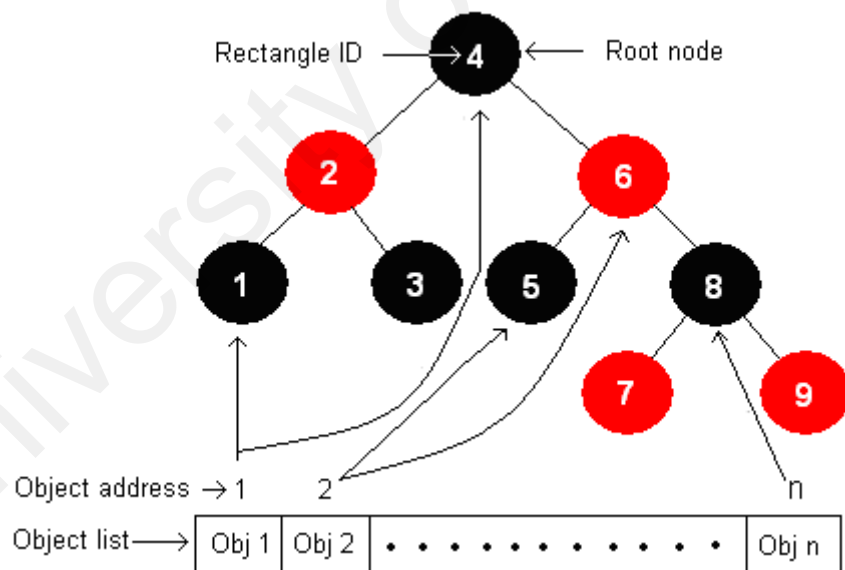


Figure 3.4: Illustrations of object address distribution technique.

The whole operation described above is done before the ray tracing process. Therefore, it does not affect the simulation time of the proposed ray tracing method.

Algorithm: Insert_In_Red_Black_Tree(Tree &root, Item_Type item, Rectangle rect)

Input: Root of the Red-Black tree

Output: True or False

1. **if** (root = NULL) **then**
2. root = **new** black node
3. root.rectangle= rect
4. **return** true;
5. **else if** (item = root.data) **then**
6. **return** false
7. **else if** (item < root.data) **then**
8. **if** (left = NULL) **then**
9. left = **new** red node
10. left.rectangle= rect
11. **return** true
12. **else if** ((left = red) && (right = red))
13. change left and right to black and color the local root red;
14. **if** (**Insert_In_Red_Black_Tree**(left, item, rect)) **then**
15. **if** (left grandchild = red) **then**
16. change left to black and color the local root red;
17. rotate the local root right;
18. **else if** (right grandchild = red) **then**
19. rotate the left child left;
20. change left to black and color the local root to red;
21. rotate the local root right;
22. **end if**
23. **if** (local root is root of the tree) **then**
24. color the root black.

Figure 3.5: Recursive small rectangle insertion function of the Red-Black tree.

3.1.3 SURFACE SEPARATION AND CALCULATION OF INTERSECTION POINT

At the beginning of ray tracing, rays are launched from the location of T_x at an angle θ . Afterwards, an intersection test is performed to identify the intersection point on an object surface. To do this easily and accurately, the surface separation technique is introduced here. Based on the quadrant of rays, the particular surfaces are separated from the 3-D objects (humans, walls, partitions, and furniture) to determine the intersection point. For example, if a ray travels into the first quadrant then this ray will possibly hit left/bottom surface of a 3-D object and thus, it will be sufficient to separate these surfaces from the 3-D object for the intersection test, as demonstrated in Figure 3.6. Similarly, for the second quadrant, right/bottom surface will be separated from a 3-D object. Top/bottom and Top/left surface will be separated from a 3-D object in the case of the third and fourth quadrant, respectively that means for each intersection test only two surface is taking part in the intersection tests, namely surface skipping technique.

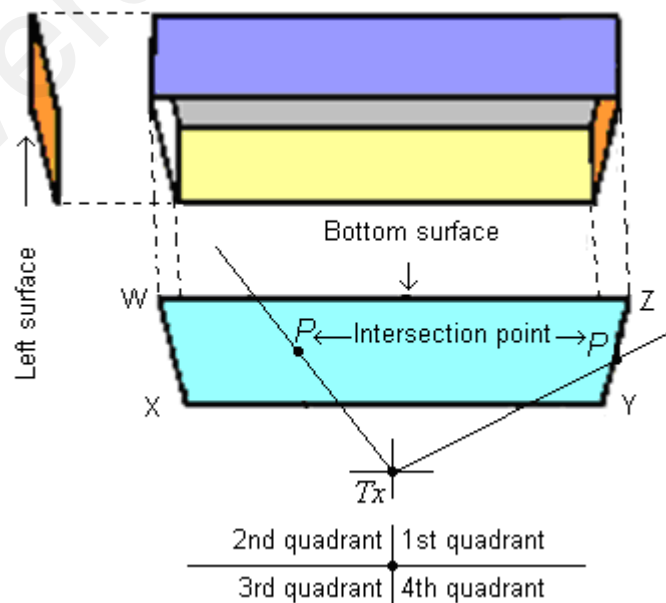


Figure 3.6: Illustration of separated surfaces of a 3-D object and intersection point.

Since, each of the separated surfaces of an object is a polygon that participates in ray-object intersection test. Referring to Figure 3.6, a ray travels into the first quadrant and another ray travels into the second quadrant with respect to its origin, and thus, the bottom surface is first separated from the 3-D object to find out the intersection point (P) on it. To determine the ray and polygon intersection, many methods can be found in the literature. The simplest way is-

- (i) Perform an intersection test between the ray and the plane containing the polygon. If the intersection point does not exist on it then finished.
- (ii) Afterward, a point-in-polygon test is needed to determine that it is inside the polygon or not.

In this study, we have ignored both these steps and directly perform the intersection test between the ray and polygon (separated surface), because we know the each coordinate of 3-D objects that are used in the simulation environment and therefore, a significant amount of intersection time are saved by the proposed method. Given a ray $P = P_0 + U\vec{V}$, originated from the $P_0(x_0, y_0, z_0)$ and if it is incident at given a polygon (separated surface) with m vertices $P_1(x_1, y_1, z_1)$ through $P_m(x_m, y_m, z_m)$ then the intersection point $P(x, y, z)$ on this ray is calculated by the following equations-

$$x = x_1 + U(x_2 - x_1) \quad (3.1)$$

$$y = y_1 + U(y_2 - y_1) \quad (3.2)$$

$$z = z_1 + U(z_2 - z_1) \quad (3.3)$$

If the surface normal of the polygon is denoted by \vec{S} and the direction vector is denoted by $\vec{V}(m, n, o)$, the intersection point between the ray and the polygon will be computed by solving the implicit equation-

$$(P - P_1) \cdot \vec{S} = 0 \quad (3.4)$$

We can get the value of scalar parameter U of the equations (3.1-3.3) by following way-

$$U = \frac{(P_1 - P_0) \cdot \vec{S}}{\vec{V} \cdot \vec{S}} \quad (3.5)$$

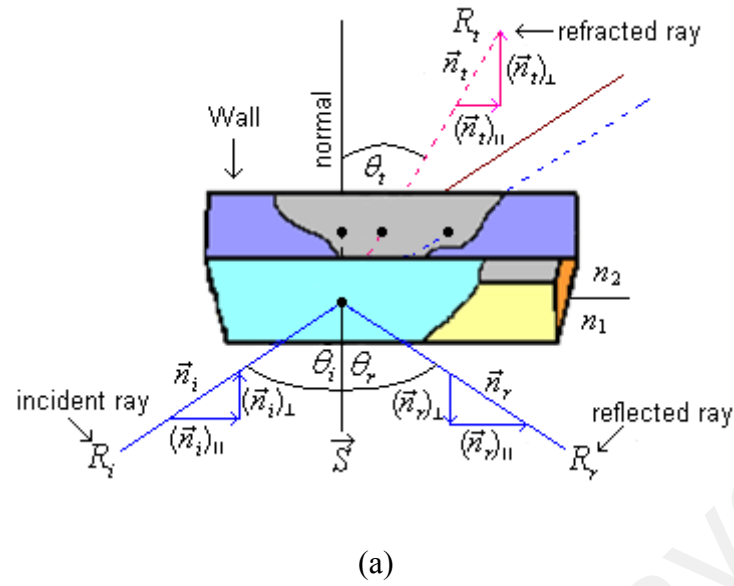
where “.” is a dot product. The intersection point P is calculated by substituting the U value of Equation (3.5) in Equations (3.1-3.3). Based on the object properties and intersection type, this point (P) will be used to build either reflected, refracted ray or diffracted ray for this simulation, as well-presented in Figure 3.5.

3.1.4 CALCULATION OF THE DIRECTION OF RAY'S

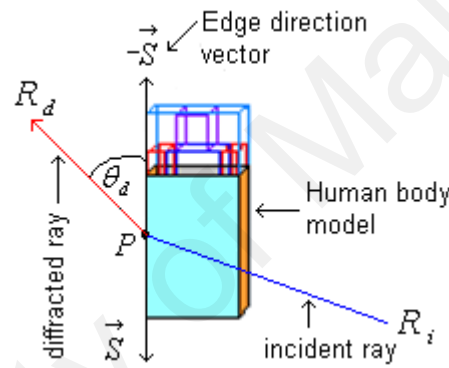
The building materials and the existed objects inside the buildings influence the indoor radio wave propagation. A simple movement of interior objects can change the entire propagation paths of reflected, refracted, and diffracted rays. Therefore, an accurate calculation is needed to determine the direction of these rays. In this study, the direction of the propagated rays will be calculated using the physics and vector geometry (Gatland, 2002; Smith, 1963). In Figure 3.7(a), ray R_i incident at point P on an object surface. The smallest positive angles of incidence, reflection and refraction, and the normal vector \vec{S} are θ_i , θ_r , and θ_t . Let \vec{n}_i , \vec{n}_r , and \vec{n}_t be the unit vectors along with the direction of incident, reflected, and refracted ray, respectively, with \vec{S} being the normal vector at point P . For any of these angles θ and any direction vector n , the desired direction of reflected ray can be calculated by the following equation-

$$\begin{aligned} \vec{n}_r &= [\vec{n}_i - (\vec{n}_i \cdot \vec{S})\vec{S}] - (\vec{n}_i \cdot \vec{S})\vec{S} \\ &= \vec{n}_i - 2(\vec{n}_i \cdot \vec{S})\vec{S} \end{aligned} \quad (3.6)$$

where “.” represents dot product.



(a)



(b)

Figure 3.7: Illustration of (a) reflection and refraction of incident ray within a wall (b) diffraction of incident ray from approximated human body model.

For the case of refracted ray, when a ray enters a denser medium it is refracted towards the normal according to the Snell's law the ratio of the sine of the angle of incidence to the sine of the angle of refraction is constant, this constant being called the *refractive index* n . According to the Figure 3.7 (a), the direction of the refracted ray-

$$\vec{n}_t = \frac{n_1}{n_2} \vec{n}_i - \left(\frac{n_1}{n_2} \cos \theta_i + \sqrt{1 - \left(\frac{n_1}{n_2} \right)^2 (1 - \cos^2 \theta_i)} \right) \vec{S} \quad (3.7)$$

On the other hand, the direction of the diffracted ray as shown in Figure 3.7(b) is calculated by the following equation (Tsingos et al., 2001)-

$$\overrightarrow{PR_i} \cdot \overrightarrow{S} = \overrightarrow{PR_d} \cdot (-\overrightarrow{S}) \quad (3.8)$$

where R_i is the origin of the incident ray, R_d is the end point of the diffracted ray, P is the intersecting point of the incident ray, and \overrightarrow{S} is the edge direction vector. Here, the edge direction vector \overrightarrow{S} is oriented such that $\overrightarrow{S} \times \overrightarrow{W} = \overrightarrow{N}$, where \overrightarrow{W} is a vector that exists on the plane of one of the two polygons of the wedge and \overrightarrow{N} is the unit vector.

3.1.5 DETERMINATION OF CLOSEST INTERSECTION POINT

When a launched ray is passed in any direction of the 3-D space, it may intersect more than one object. Therefore, it is needed to find out the closest object intersection of the ray. To do this, the closest intersection can be calculated by the following procedure:

Algorithm: Find_CIP(Ray,TreeNode, CIP)

Input: Ray and particular Red-Black tree node

Output: Closest intersection point

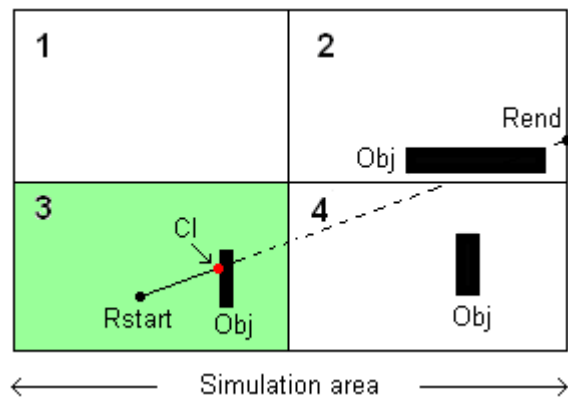
// Initialization

1. minDist \leftarrow **GetDistance**(Ray.StartLocation, Ray.EndLocation)
2. **foreach**(Object in TreeNode)**do**
3. intersectionPoint \leftarrow **Find_IP**(Ray, Object)
4. **if** (intersectionPoint \neq Empty) **then**
5. dist \leftarrow **GetDistance**(Ray.StartLocation, intersectionPoint)
6. **if** (dist < minDist) **then**
7. minDist \leftarrow dist
8. CIP \leftarrow intersectionPoint
9. **end if**
10. **end if**
11. **end for**

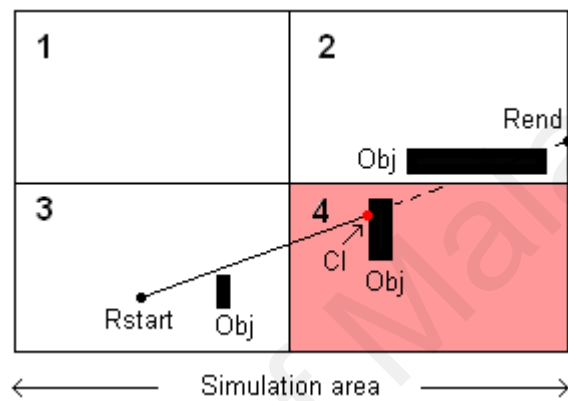
// Return closest intersection point (CIP)

12. **return** CIP

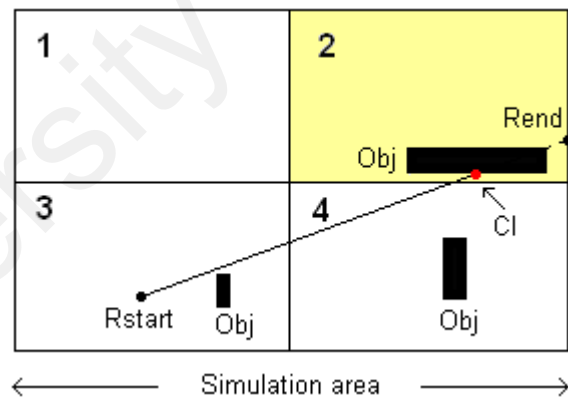
Figure 3.8: Closest intersection point (CIP) detection within a single rectangle.



(a)



(b)



(c)

Figure 3.9: Closest intersection point detection based on the valid rectangle detection.

- (i) By using the algorithm stated in Figure 3.8, perform intersection tests between the ray ($Rstart$) and objects that exist in the rectangle (R3) from where this ray is originated as shown in Figure 3.9(a). If any intersection found in the origin rectangle then skip the next step.

- (ii) Otherwise, perform intersection tests (using algorithm stated in Figure 3.10) between this ray and rectangles (stored in the Red_Black tree as demonstrated in Figure 3.4) for searching the valid rectangles (2 and 4). Valid rectangle means, those rectangles that contain objects and must intersect with the emanated ray. Once rectangles are found, store them in a list as first nearest rectangle 4 in first position, and then second nearest rectangle 2 in second positions and so on. For finding the closest intersection point (*CI*), retrieve the objects from the object list (as predicted below in Figure 3.4) by using the object addresses stored in the first nearest rectangle 4 as presented in Figure 3.9(b). The ray (*Rstart*) does not intersect with the object in the rectangle 4 and therefore, object in the second nearest rectangle 2 is take part in intersection tests for finding the closest intersection point (*CI*) as presented in Figure 3.9(c).

Algorithm: Find_CIP_In_Valid_Cell(Ray, RB_Tree)

Input: Ray and Red-Black tree

Output: Closest intersection point

// Initialization

25. CIP \leftarrow 0.0

26. **foreach**(TreeNode in RB_Tree) **do**

27. **if**(Valid(TreeNode)) **then**

// Call the algorithm stated in Figure 4

28. CIP \leftarrow **Find_CIP**(Ray,TreeNode, CIP)

29. **end if**

30. **end for**

// Return closest intersection point (CIP)

31. **return** CIP

Figure 3.10: Closest intersection point (CIP) detection within valid rectangles.

If multiple intersections are found within a single rectangle as shown in Figure 3.11 then the closest intersection point (CI_1) can be identified based on the distance from the ray's emanating point.

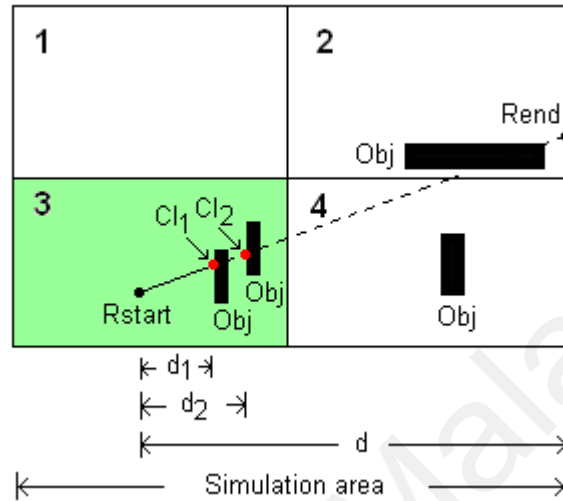


Figure 3.11: The closest intersection point CI_1 identified based on the distance from the ray's emanating point.

Referring to Figure 3.11, a ray starts at R_{start} and ends at R_{end} . This ray intersects with two objects at CI_1 and CI_2 , respectively. According to the closest distance of origin of the ray, CI_1 is the closest intersection of this ray, because the distance between R_{start} and CI_1 is closer than the distance between CI_2 and R_{end} , that is, $d_1 < d_2 < d$.

3.2 RAY TRACING METHOD

In the proposed simulation, human body is presented like a wall, partition or furniture with identical surfaces, and these surfaces could reflect, refract, and diffract the propagated waves. The simulations are carried out by change of the location of each movable object (human). Initially, all objects are placed in their desired locations of the simulation space, where each object has a fixed location. Among these objects, only the location of the movable objects (human) is modified by the predefined speed and

direction before the simulation. Afterwards, the simulation results will be obtained by a regular time interval, which will provide the ability to recompute the simulation parameters and current location of the moving objects.

For ray tracing in a particular time interval, this study considers an indoor environment, as presented in Figure 3.10. According to the space splitting technique, the simulation area is divided into six similar sized rectangles, the ID's (1 through 6) of which are enclosed by the red background rectangles, as shown in Figure 3.12. Information of these rectangles and corresponding object addresses are kept in a Red-Black tree, as mentioned in Section 3.1.2. Ray tracing begins with launching rays in each possible direction in the simulation space.

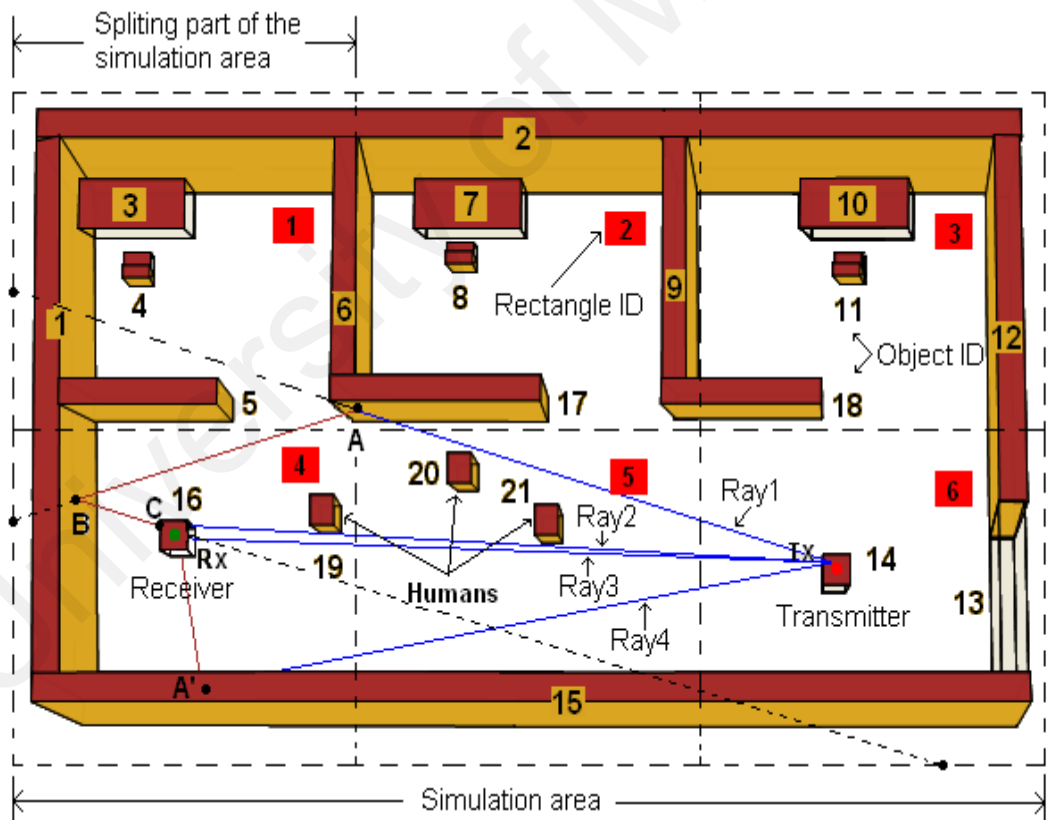


Figure 3.12: Illustration of the proposed ray tracing in an indoor environment.

After building a ray, the travelling quadrant of the launched ray is calculated by using the incident angle θ . When the incident angle θ is in between 0-90, 91-180, 181-270,

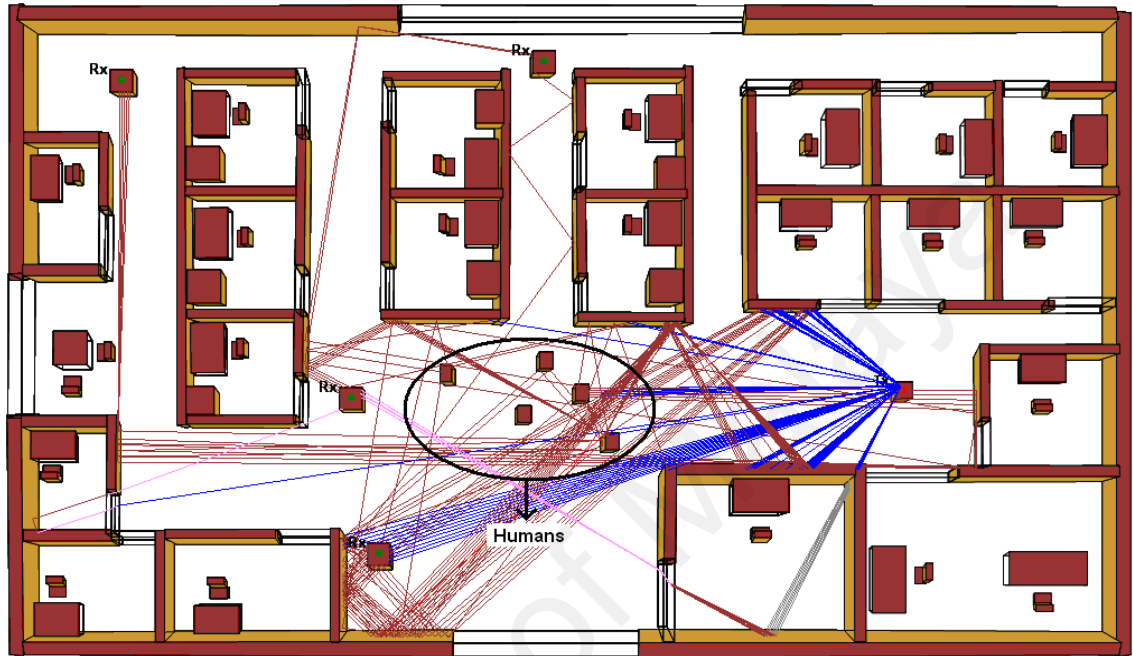
and 271-359 degrees then this ray will travel the first, second, third, and fourth quadrant, respectively. In Figure 3.12, the transmitter and receiver are placed in the Rectangle 6 and Rectangle 4, respectively. It is clear that, four significant rays reached the receiver by multiple reflections and each ray composed of multiple ray segments. For instance, Ray 1 is formed by three ray segments TxA , AB , and BRx . To efficiently build up the ray segment TxA , the proposed algorithm first calculated the travelling quadrant of the ray segment TxA . Then, based on the procedure (i) stated in previous section, it performs the intersection tests between the ray segment TxA and objects exist in the Rectangle 6. During the intersection test, particular surfaces are taken out one after another from the retrieved objects based on the surface separation technique as described in Section 3.1.3. After that, intersection test has been done between this ray and separated object surface. It can be seen from Figure 3.12 that, Ray1 does not intersect with any object exists in the Rectangle 6. Therefore, the procedure (ii) is applied to find out the closest intersection point A. According to the procedure (ii) as described in the previous section, a search operation is performed within the Red-Black tree for finding the valid rectangles. In this situation, Rectangle 1, Rectangle 2, and Rectangle 5 are the valid rectangles, because they are intersected with the ray segment TxA . Afterward, objects exist in the Rectangle 5 have to retrieve from the object list by using the object addresses stored in the valid Red-Black tree nodes of valid Rectangle 5. In this case, Ray 1 does not intersect with any object exists in this rectangle and therefore objects in Rectangle 2 have to retrieve from the object list by using object addresses stored in Red-Black tree node 2. After applying procedure (i) presented in previous section, the closest intersection found on the object 17 and it will stop the search procedure. It can be seen from Figure 3.12 that, only 12 objects (2, 6, 7, 8, 9, 12, 13, 15, 17, 18, 20, and 21) are taking part in the intersection test. Based on the object property and intersection type, this intersection point is used as an origin of the

reflected, refracted or diffracted ray. The reflected ray is generated, when the ray segment hits the object surface. Diffracted ray is generated when the ray segment hits the sharp edge of an object, and refracted ray is generated when the ray hits the transparent objects. It is evident that, the ray segment TxA hits the object surface, which is not a receiver and thus, a new ray segment AB has to be built. The direction of the reflected, refracted, and diffracted ray is calculated by using Equations (6), (9), and (10), respectively. To build up the ray segment AB , the proposed algorithm sequentially follows the procedure (i) and (ii). For the ray segment AB , only 9 objects (1, 2, 3, 4, 5, 6, 15, 16, and 19) are taking part in the intersection test and the closest intersection point B found on object 1. A new reflected ray BC has to build from the closest intersection point B . Therefore, the proposed algorithm applies the procedure (i) to find out the closest intersection point C . In this case, only 4 objects (1, 15, 16, and 19) exist in the Rectangle 4 are taking part in the intersection test. The ray segment BC intersects with the receiver, therefore, the entire ray path is considered as a significant ray path that originates from the transmitter and reached the receiver after multiple reflections. Therefore, another ray is needed to launch from the position of Tx to trace the next ray and so on.

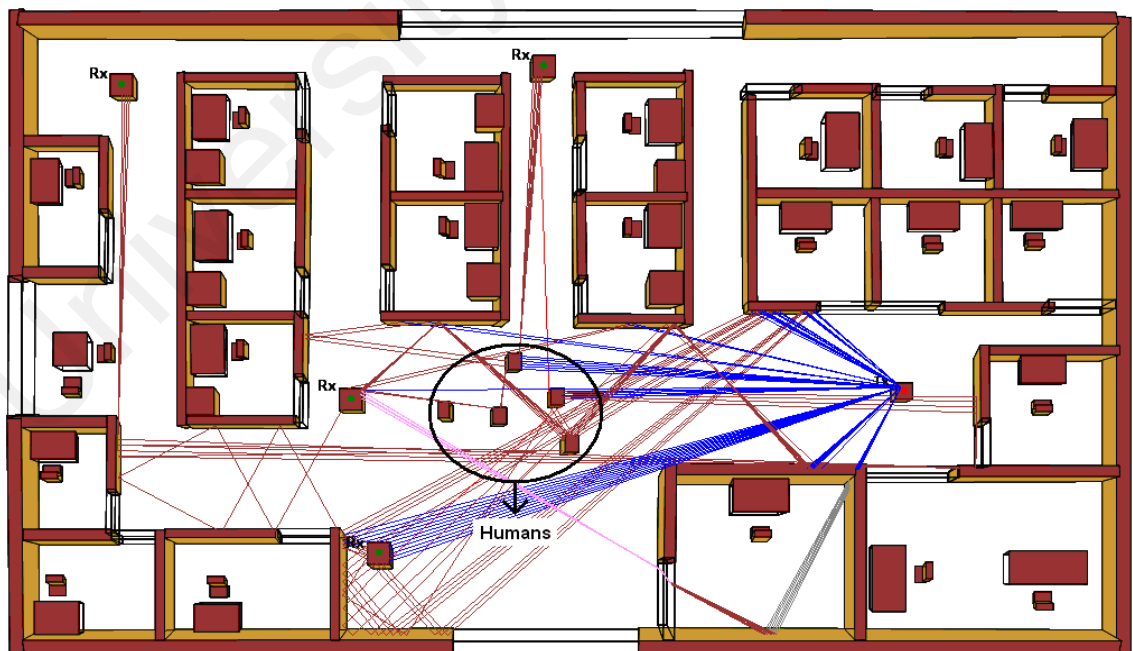
In general, an intersection point can be found by testing each object surface of an indoor environment. Therefore, a total of $21*6=126$ intersection tests are needed to find a single intersection point for the general ray tracing algorithm. Finally, 3 intersection points are needed to find the Ray 1 and thus, at least $(3*126) = 378$ intersection tests are required for the general ray tracing algorithm. Conversely, a total of $(24+18+8) =50$ intersection tests is needed for the Ray 1 by using the proposed ray tracing algorithm because of the object address distribution and surface skipping techniques.

Figure 3.13 shows two different rays tracing scenarios (Figure 3.13(a) taken from the initial location of movable objects and Figure 3.13(b) taken by automatically moving

the movable objects in other locations) generated by the proposed ray tracing method. In Figure 3.13, the labeled by Tx and Rx represent the transmitter and receiver, respectively and objects within the black circle are the humans. It can be observed from Figure 3.13(a) that 67 significant signals reached the receivers.



(a)



(b)

Figure 3.13: Illustration of ray tracing (a) when movable objects are placed at their initial locations (b) after automatically moved to the new locations.

Algorithm: Ray_ Tracer (StartingAngle, RB_Tree, Tx, ObjectList)

Input: Random angle, Red-Black tree, Information of Tx, and List of objects

Output: Draw only the significant Ray's

// Initialization

1. Angle \leftarrow StartingAngle
2. Ray.StartLocation \leftarrow Tx.StartLocation
3. Ray.OriginTreeNode \leftarrow Tx.OriginTreeNode

// Find significant rays

4. **repeat**
5. Ray.Object \leftarrow Null
6. Valid_Tree_Nodes \leftarrow new Red_Black_Tree()
7. Quadrant \leftarrow FindQuadrant (Angle)
8. Ray \leftarrow CreateRay (Quadrant, Ray.StartLocation)
9. Ray \leftarrow FindClosestIntersectPoint (Ray, ObjectList)
10. Ray.Type \leftarrow IncidentRay
11. **if** (Ray.EndLocation = 0.0) **then**
12. Valid_Tree_Nodes \leftarrow FindValidRectangles (Ray, Red_Black_tree)
13. **foreach** (RB_Tree TreeNode in V_Tree_Nodes) **do**
14. Ray \leftarrow FindClosestIntersectPoint (Ray, TreeNode, ObjectList)
15. **if** (Ray.EndLocation !=0.0) **then**
16. Ray.OriginTreeNode \leftarrow TreeNode
17. **break**
18. **end if**
19. **end foreach**
20. **end if**
21. ListOfRay.Add(Ray)
22. Ray.IncidentAngle \leftarrow CalculateAngleOfNextRay(Ray.IncidentAngle)
23. Ray.Type \leftarrow CalculateTypeOfNextRay(Ray.EndLocation,Ray.Object)
24. Ray.StartLocation \leftarrow Ray.EndLocation
25. **until** (Ray.Power > ThresholdPower)

// Draw significant rays only

26. **if** (ListOfRay[ListOfRay.Count - 1].Object == "Receiver") **then**
27. DrawOnlySignificantRays(ListOfRay)
28. **end if**

// Choose an appropriate angle and recall the ray tracer again

29. StartingAngle \leftarrow ChooseAnAngle(StartingAngle)
 30. **if** (StartingAngle.Count <= ThresholdValue) **then**
 31. Ray_ Tracer (StartingAngle, RB_Tree, Tx, ObjectList)
 32. **end if**
-

Figure 3.14: Proposed recursive ray-tracing algorithm.

However, 57 significant signals reached the receivers (as shown in Figure 3.13(b)) by following different propagation paths when the humans have changed their location. The proposed ray tracing method is projected in Figure 3.14.

3.3 COMPLEXITY ANALYSIS

The proposed method uses object address distribution technique along with Red-Black tree data structure for the optimization of ray tracing time, where a significant amount of ray tracing time can be minimized by using the Red-Black tree. Because, the computational complexity for insertion, deletion or searching of an object can be shown to be $O(\log_2 N)$. Based on this, the time complexity of the proposed method is given below.

According to the object address distribution technique, if N number of objects is uniformly distributed over the simulation area, then on average N' number of objects exist in a particular rectangle R , where R is the number of splitting parts (rectangles) of the simulation space stored in the Red-Black tree. Therefore, N' number of objects has-

$$S = N' \times s \quad (3.9)$$

surface planes, where s is the number of surfaces of each object. The average number of objects N' can be calculated using the following equation-

$$N' = N/R \quad (3.10)$$

If r intersections are involved to predict each significant ray then the computational complexity of the proposed method is calculated by the following equation-

$$r \times O(\log_2 R + S) \quad (3.11)$$

In this study, the surface skipping technique is applied to leave out the unnecessary object surface and thus, it reduces the ray tracing time. Therefore, if s' number of

surfaces out of a total s number of surfaces takes part in intersection tests, then the total number of surface planes can be expressed as-

$$S' = N' \times s' \quad (3.12)$$

Finally, using Equations (3.11) and (3.12), the time complexity of the proposed method can be expressed as-

$$r \times O(\log_2 R + S') \quad (3.13)$$

On the other hand, ray tracing model in (Khafaji, 2008) is developed to demonstrate the effect of human movement on wave propagation in a typical indoor environment. Here, the ray tracing algorithm (based on image method) (McKown and Hamilton, 1991) is used for the characterization of the radio wave propagation. Hence, time complexity of the image method for the r number of reflections, can be expressed as (Zhihua et al., 2009)-

$$O(S^r) \quad (3.14)$$

Where, $S = (N \times s)$ surface planes in an environment. Moreover, another model described in (Genc et al., 2012) is also used to investigate the characteristics of the radio wave propagation in a living room under the influence of human movement. The RL algorithm is used in the ray tracing simulator that also involved to characterized wave propagation in indoor environments. However, the time complexity for the r number of reflections of the RL method is-

$$r \times O(S) \quad (3.15)$$

Because, every surface plane ($S = N \times s$) is involved in the ray-object intersection test.

One of the earlier techniques to reduce the number of ray-surface intersection tests is the Space volumetric partitioning (SVP) method (Catedra, 1999). According to (Catedra, 1999), the 3-D space surrounding the environment is divided into voxels. All the voxels together constitute a volume that contains the environment. For each voxel, the surfaces

that lie totally or partially inside are determined. This information is stored in the SVP matrix, which will be interrogated repeatedly in the intersection tests. According to this algorithm, let, the simulation space is divided into R voxels and stored in a matrix M . During the intersection test, SVP method search for a desired voxel among the R voxels, which needs-

$$O(R) \tag{3.16}$$

computational time in worst case. If on average N' number of objects exists in each voxel then it can be calculated by using the following equation-

$$N' = N/R \tag{3.17}$$

For r number of reflections, the worst case time complexity of the SVP method is calculated by the following equation-

$$r \times O(R + S') \tag{3.18}$$

where, $S' = N' \times s$.

Another accelerated ray tracing method namely Angular Z-Buffer is presented in (Catedra, 1999; Chiya and H., 2010). For a given source (S), the AZB technique divided the simulation space into some angular regions. Using an arrangement similar to the SVP method, they are called *anxels* as an abbreviation for angular elements. Afterwards, the surfaces of the scene that lie in each *anxel* are determined. The information about the *anxel* and corresponding surfaces is stored in the AZB matrix. According to this method, the number of angular region (A_r) is calculated by the following equation-

$$A_r = \frac{360}{anxels} \tag{3.19}$$

During the intersection tests, this method retrieves the surfaces from the angular region A_R that are stored in AZB matrix M . For r number of reflections, AZB method spends-

$$r \times O(A_R + S')$$
 (3.20)

time in worst case, where S' is the number of surfaces in a particular angular region. In order to compare the proposed and existing methods, a comparison of time complexity is projected in Table 3.1.

Table 3.1: Time complexity of the proposed and existing (Catedra et al., 1998; Genc et al., 2012; Khafaji, 2008) ray tracing algorithms.

Algorithm	Worst case time complexity
Image method (Khafaji et al., 2008)	$O(S')$
RL method (Genc et al., 2012)	$r \times O(S)$
SVP method (Catedra, 1999)	$r \times O(R + S')$
AZB (Chiya and H., 2010)	$r \times O(A_R + S')$
Proposed method	$r \times O(\log_2 R + S')$

It is obvious that, the time complexity of the proposed method is much better than the time complexity of the existing methods, because of the Red-black tree data structure, object address distribution, surface skipping and smart object searching techniques as described earlier.

CHAPTER 4

RESULTS AND DISCUSSION

The simulation environment for the proposed method has been implemented over visual studio 2008 using C sharp Object Oriented Programming, running on 2.99 GHz Pentium IV processor with 1GB memory. The operating system is Microsoft XP. The results for various scenarios are compared in the same hardware configuration. The result and discussion part is divided into two subsections. Since, the main goal of this study is to developed an efficient algorithm that enough for sufficiently accurate simulation. Therefore, to prove the superiority of the proposed method, a comparison based on the ray prediction accuracy (based on predicted rays), ray prediction time will present in the first subsection and the impact of the human movement on the received rays, computation time and received power will present in the next subsection.

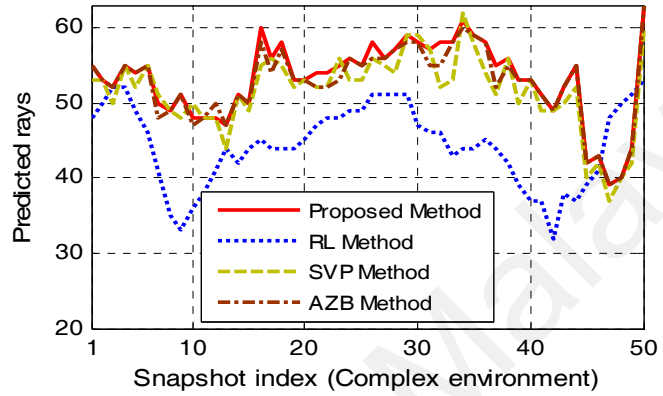
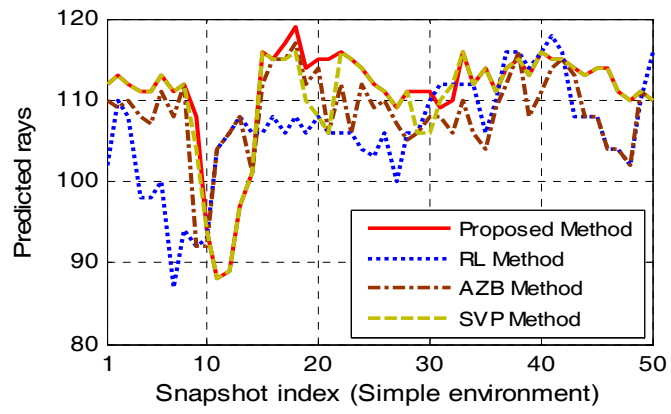
4.1 PERFORMANCE EVALUATION

The proposed method is compared with the image (Khafaji et al., 2008), RL (Genc et al., 2012), SVP (Catedra, 1999) and AZB (Chiya and H., 2010) methods. All simulations have been done for two different environments; first one is a simple environment as shown in Figure 3.12 and the second one is a very complex environment as shown in Figure 3.13. The obtained results confirm the precedence of the proposed algorithm. The image method is accurate, because it is able to predict all the specular paths up to a given order will be found. Conversely, it suffers from inefficiency when the number of objects involved is large and there are many reflections for a single path from transmitter to receiver, this method suffers from large computation time. On the other hand, the accuracy of the ray launching method is greatly reduced for those rays traveling long distances from the transmitter. In these situations, such ray tracers may

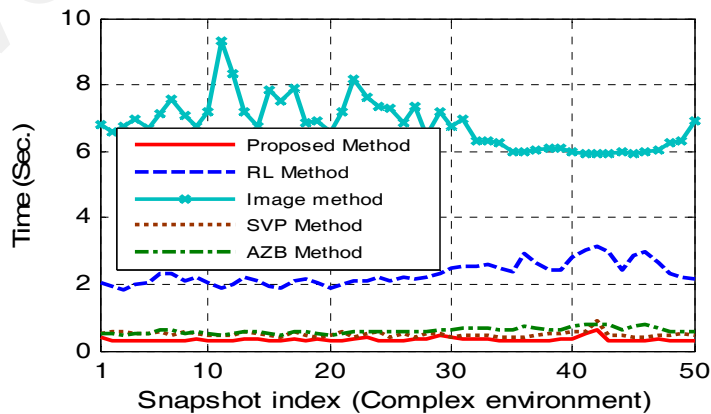
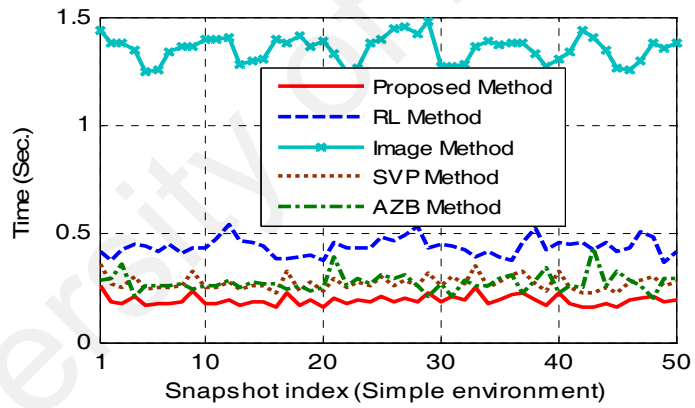
miss important interactions and thus, it can be said that, the ray launching technique is suffering from accuracy in terms of ray prediction.

The proposed method is developed for better performance with respect to both ray prediction accuracy and computational efficiency. It can predict all specular paths up to a given order because of rays are launched in each possible direction in the 3-D indoor environment. Moreover, the proposed method first searches the Red-Black tree for finding valid rectangles then objects exist within these rectangles and only two surfaces of each object take part in the intersection test. Therefore, none of the intersections have been missing during the intersection tests, which ensure that the proposed method is more accurate than the existing methods. On the other hand, the computation time of the proposed method remains at minimum level because of the object address distribution and smart object searching techniques as mentioned in subsection 3.1.2 and 3.1.5, respectively. In addition, it can be said from the complexity analysis section, the proposed method can reduce huge amount of ray prediction time compared to the existing ray tracing methods used in (Catedra, 1999; Chiya and H., 2010; Genc et al., 2012; Khafaji et al., 2008).

As the accuracy (number of predicted rays) is same as the image and SVP methods, Figure 4.1 shows a comparison, which is based on the predicted rays and corresponding computation time that considers a human body moving parallel to the line-of-sight (LOS) paths in two different indoor environments as shown in Figure 3.12 and Figure 3.13, respectively. And, the average value of the predicted rays of each method is presented in Table 4.1. It is observed from Figure 4.1(a) and Table 4.1 that, the proposed method predicts the higher amount of rays compared to the RL (it is about on average 4% and 16%) and AZB (it is about on average 2.28% and 2.67%) methods, when the simulation was carried out in a simple and complex indoor environment, respectively.



(a)



(b)

Figure 4.1: (a) Ray prediction and (b) corresponding computation time for the proposed and existing ray tracing methods, which is obtained from two different indoor environments.

These percentages of predicted rays can be calculated by the following equation-

$$\frac{Rays_{proposed} - Rays_{existing}}{Rays_{proposed}} \times 100 \quad (4.1)$$

Table 4.1: Average ray prediction result of the proposed and existing ray tracing algorithms.

Algorithm	Ave. Rays (Simple Env.)	Ave. Rays (Complex Env.)
Image method (Khafaji et al., 2008)	111	53.08
RL method (Genc et al., 2012)	106.42	44.42
SVP method (Catedra, 1999)	110.28	52.58
AZB (Chiya and H., 2010)	108.46	51.66
Proposed method	111	53.08

According to Figure 4.1(b), the proposed method is 69.30% and 91.47% (on average) faster than the RL and image methods, when the simulation was carried out in the simple and complex indoor environment, respectively. The SVP method spends 29% and 32.5% more computational time than the proposed method for simple and complex indoor environment, respectively. Because, the only surfaces that must be tested for intersection are those stored in the voxels matrix pierced by the ray and search operation of those surfaces from voxels matrix follow the linear search time instead of the logarithmic search time. Conversely, the AZB method takes almost same amount of computational time with the SVP method in the case of the simple indoor environment while takes additional 14.95% computational time for the complex indoor environment. For a given number of anxels, the efficiency of the angular partitioning decreases when the size of the scene increases. This is because far away from the source, the area that occupies each anxel will be large so it could contain a large number of surfaces and therefore increases the computational time. Moreover, it can be observed from Figure 4.1(b) that, the proposed method relatively obtaining the constant time for two different

environments and the simulation time does not directly follow the number of objects in the indoor environment.

4.2 EFFECT OF HUMAN MOVEMENTS

To demonstrate the human movement effect on the received rays and subsequent computation time, this study considers a single floor of dimension $20\text{ m} \times 32\text{ m}$ having multiple furnished rooms as shown in Figure 4.2. During the simulation, this study considers the Tx and Rx are remains stationary, with the distance of 5 m in between them, and humans randomly arrive and penetrate the LOS along a straight path as shown in Figure 4.2 at a constant speed (modifiable) is about 2.5 cm/s .

The presented human body model as illustrated in subsection 3.1.1 is used to simulate the human activity in the indoor environments.

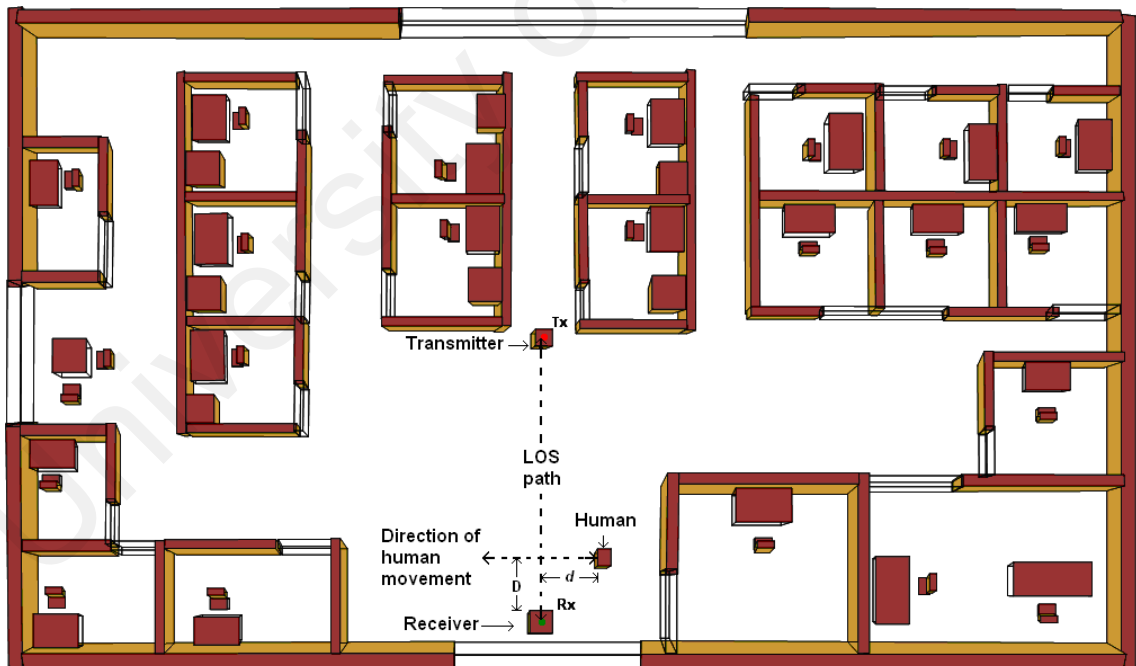


Figure 4.2: Model of LOS blocking by a human body in a complex indoor environment.

The reflection and transmission coefficient is calculated from the general equations (Pena et al., 2003) and the diffraction coefficient of the proposed and existing methods is calculated by using well known Uniform Theory of diffraction (UTD) (Tsingos et al., 2001). A semi-spherical antenna operating at 60 GHz with 15 dB gain and radiating 10mW is used as the T_x . At the receiver side, same type of antenna is used. Detailed specifications of the indoor environment used in the proposed simulation software are given in Table 4.2.

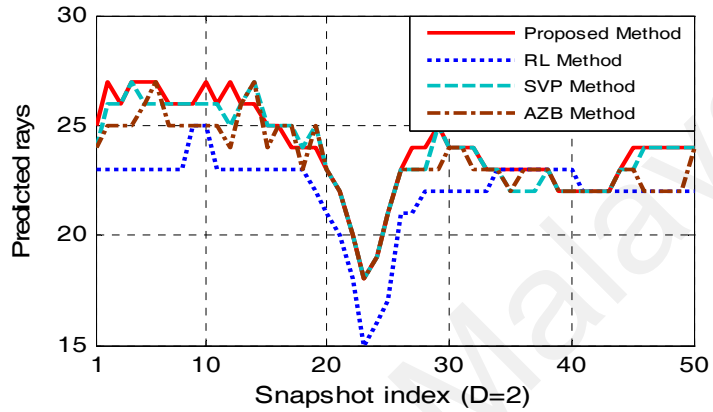
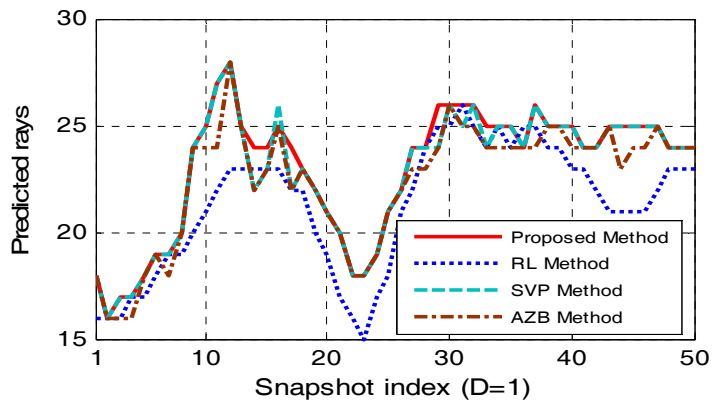
Table 4.2: Specification of the simulation environment.

Name	Materials	Height	Width	Thickness	Permittivity (ϵ_r)
Human	Human body	1.70 m	0.56 m	0.305 m	1.0
Outer wall	Brick	2.8 m	-	0.21 m	5.2
Outer wall	Glass	2.8 m	-	0.21 m	3.0
Inner wall	Brick	2.8 m	-	0.1 m	5.2
Door	Glass	2.8 m	-	0.04 m	3.0
Table	Wood	0.9 m	-	0.04 m	3.0

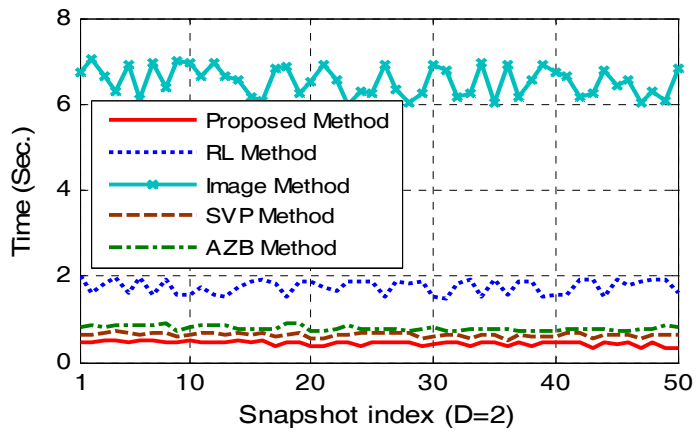
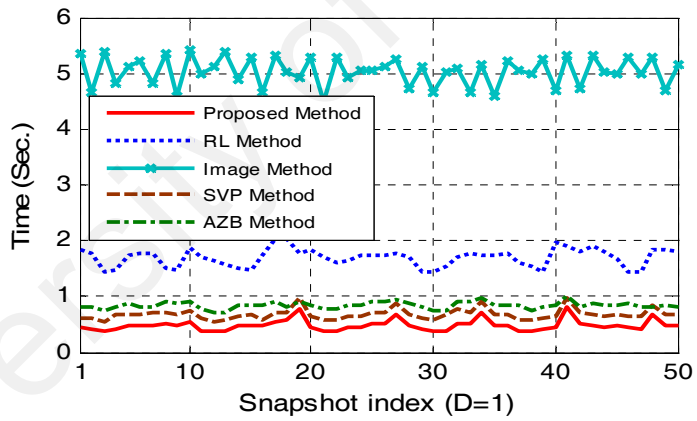
4.2.1 EFFECT OF SINGLE HUMAN MOVEMENTS FOR DIFFERENT DISTANCE BETWEEN HUMAN AND RX

To investigate the effect of single human movements for different distance between human and Rx, simulations are taken at a series of positions along the path perpendicular to the LOS. The sampling starts at $d = 1$ m and ends at 1 m on the other end of the path.

In order to show the different situations on the received rays and their computation time for the proposed and existing ray tracing algorithms used in (Catedra, 1999; Chiya and H., 2010; Genc et al., 2012; Khafaji et al., 2008), the results for a single human moving



(a)



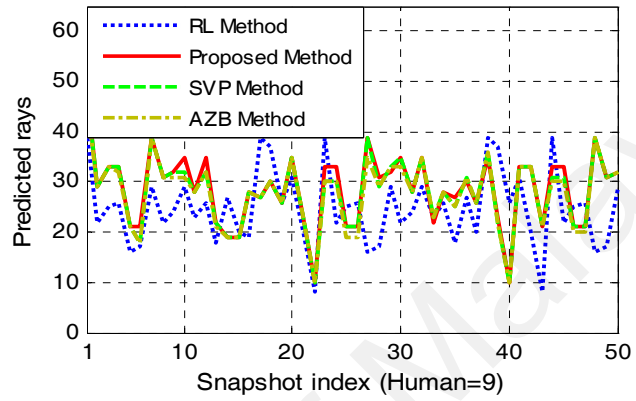
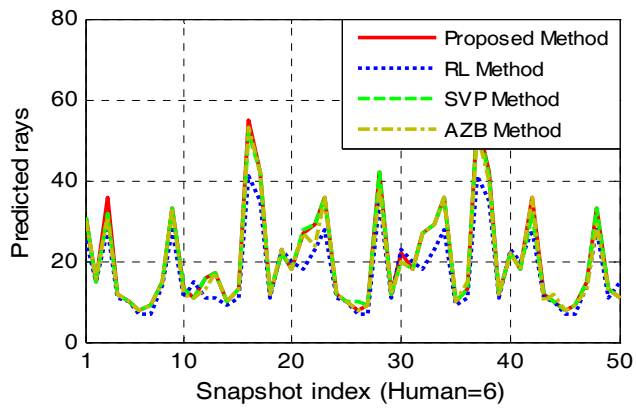
(b)

Figure 4.3: (a) Received rays and (b) their computation time variations due to the moving human for different distances between the human and R_x .

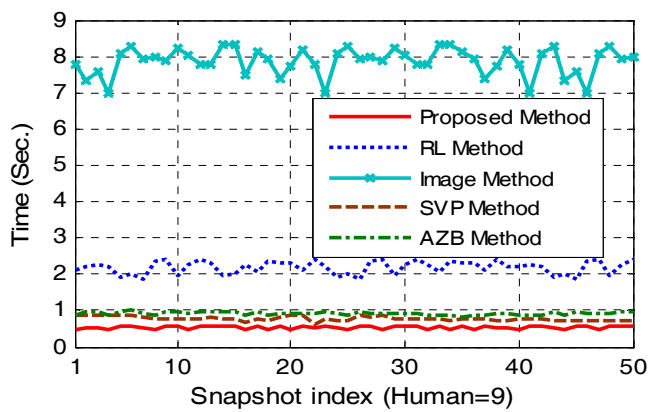
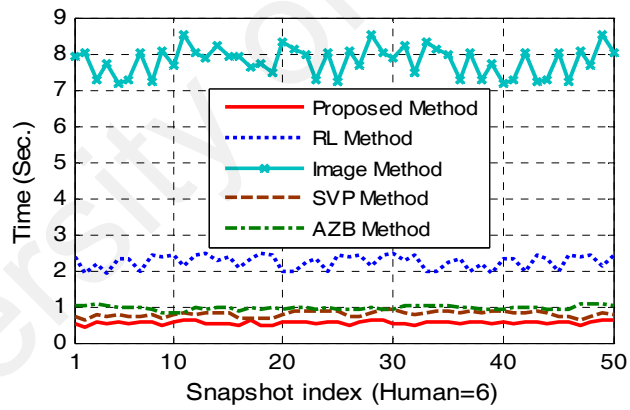
along a path with different distance D from receiver (R_x) are calculated and plotted in Figure 4.3. It can be observed from Figure 4.3(a), snapshot index 15 to 25 corresponds to the situation that the center of the human is on the LOS, therefore the received rays are rapidly fall down, and large variations on the received rays are obtained for different distances between the human body and R_x . The obtained results also show that the proposed method always predicts the higher amount of rays than the RL and predicts almost the same amount of rays as the image, SVP, and AZB methods. Conversely, it can be observed from Figure 4.3(b) that the existing methods took more time than the proposed method. Moreover, deviations on computation time are obtained (as shown in Figure 4.3(b)) when the distance between human and R_x is changed from 1 meter to 2 meters while the computation time remains constant for the proposed method. Therefore, we may summarize that the human body movement at different distances between human and R_x has less effect on the computation time of the proposed method due to the object address distribution, surface skipping, and smart object search techniques.

4.2.2 EFFECT OF THE MULTIPLE HUMAN MOVEMENTS

A comparison based on the ray prediction and computation time for different human movements is shown in the Figure 4.4, where multiple human movements in the indoor environment are taking into account. This simulation result is also taken from the indoor environment as shown in Figure 4.2. To show the different situations on the received rays for different ray tracing algorithms, the results for multiple human moving randomly with different distance from receiver (R_x) are calculated here. Figure 4.4 illustrates the behavior of the received rays and computation time versus the number of humans in the indoor environment.



(a)

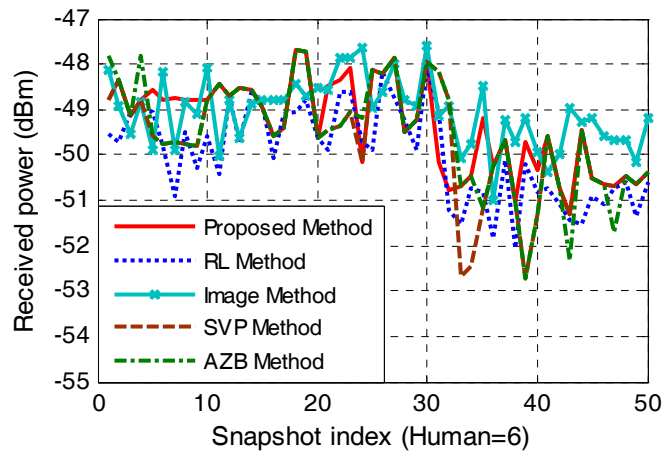


(b)

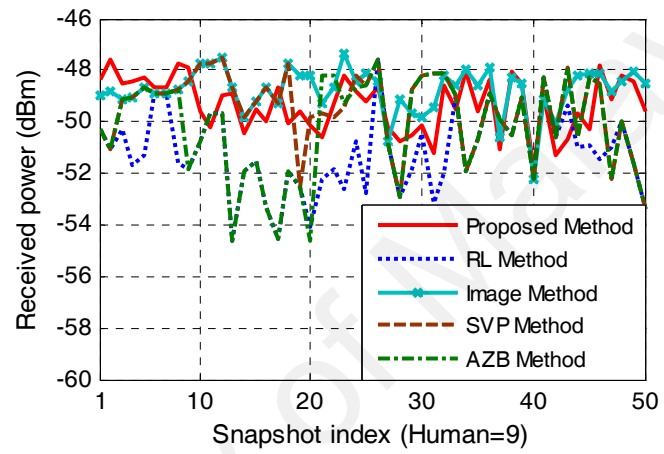
Figure 4.4: (a) Received rays and (b) their computation time variations for the multiple humans are moving parallel or perpendicular to the LOS path.

From this figure, it can be observed that the predicted rays for the proposed method increases with the number of humans compared to the RL method while the same amount of rays predict with the other three methods, as shown in Figure 4.4(a). Conversely, the computation time remains same with the different number of humans as shown in Figure 4.4(b). The reason is that, the proposed method launched rays in each possible direction and predicates all significant propagation paths that we already described in the subsection 4.1. Moreover, a new comparison based on the received power predicted in Figure 4.5, where different number of human movements are taking into account. It can be observed from Figure 4.5 that, the proposed method predicts almost the same amount of received power as image method, when six and nine humans moving in the parallel and perpendicular of the LOS path, respectively.

On the other hand, better predictions of the received power are obtained for the both cases compared to the RL method. Since, most of the rays reached the receivers through multiple reflections, refractions, diffractions and contributes to the received power in indoor environments. These rays may follow the different propagation paths based on the technique used in the different ray tracing algorithms. Therefore, differences on the received rays are observed for the different ray tracing algorithms that also makes a difference on the received power. According to Figure 4.5(a), the proposed method predicts almost same amount of the received power as image, SVP, AZB methods while better prediction result obtained in case of the RL method, when six humans are moving in parallel and perpendicular to the LOS path. On the other hand, the proposed yields almost same prediction results with the image and SVP methods, whereas better received power is obtained compared to the RL and AZB methods as shown in Figure 4.5(b), when nine humans are moving in parallel and perpendicular to the LOS path.



(a)



(b)

Figure 4.5: Comparison based on the received power for different number of humans (a) for six humans (b) for nine humans, when they are moving parallel or perpendicular to the LOS path.

CHAPTER 5

CONCLUSION

5.1 OVERALL CONCLUSION

In this study, an accelerated and accurate ray tracing method is proposed for the real life indoor environment, which is able to estimate the human movement effect on the received signals in a specific scenario of indoor environments. In this study, surface separation combined with accurate calculations of direction of reflected, refracted, and diffracted rays are used for correct ray path prediction of the transmitted rays. The proposed method launches the rays in each possible direction and used a faster object searching technique based on the object address distribution. As a result, none of the intersections are missed during the ray tracing and thus the minimal computation time is consumed by the proposed method for sufficiently accurate simulation. For reducing the ray-surface intersection testing time, the surface ignoring technique is also presented in this study.

In order to prove the superiority of the proposed ray tracing method, this study compares the proposed method with the image and RL methods as well as with faster ray tracing methods (such as SVP and AZB methods). A comparison based on number of predicted rays and ray prediction time has been obtained from a simple and complex environment and found that the proposed method predict 4% and 16% more rays than the RL method while 2.28% and 2.67% more rays than the AZB method, respectively. On the other hand, the proposed method is 69.30% and 91.47% (on average) faster than the RL and Image method, respectively. In case of simple and complex environment, the proposed method took 29% and 32.50% less time than the SVP method. On the other hand, AZB method took 29% more time than the proposed method when the

simulation is done in the simple environment while it spends 43.95% more time than the proposed method in complex environments.

To investigate the effect of single human movements for different distance between human and Rx, simulations are taken at a series of positions along the path perpendicular to the LOS and found that large variations on the received rays are obtained for different distances between the human body and Rx. Conversely, the existing methods took more time, deviations on computation time are obtained when the distance between human, and Rx is changed from 1 meter to 2 meters while the computation time remains constant for the proposed method.

A comparison based on the ray prediction and computation time for different number of humans is presented in comparison part, where multiple human movements in the indoor environment are taking into account. It is observed that the predicted rays for the proposed method increases with the number of humans compared to the RL method while the same amount of rays predict with the other three methods. Conversely, ray prediction time increases with the number of humans for the existing methods while it remains same for the proposed method. Finally, the proposed method predicts almost the same amount of received power as image, SVP, and AZB methods, when six humans are moving in parallel and perpendicular to the LOS path. On the other hand, the proposed method yields almost same prediction results with the image and SVP methods, whereas better received power is obtained compared to the RL and AZB methods, when nine humans are moving in parallel and perpendicular to the LOS path. According to the prediction results, we may conclude that the proposed method achieves the best performance for the two given indoor environments.

The proposed ray tracing method presented in this study can be effectively used to characterize the wave propagation (at millimeter band frequencies) in a given realistic single stored having multiple furnished room indoor environment.

5.2 RESEARCH CONTRIBUTIONS

Efficient and accurate characterization of the radio wave propagation in the presence of human motion is one of the most important requirements for the effective design, assessment and installation of an indoor wireless network. It enables the designer or user to predict signal coverage, to determine the optimal location for installation of antennas and to predict the performance of the system. In order to develop and implement such an efficient model, the followings are the main contributions of this dissertation:

- (i) This study developed a new 3-D human body model, namely approximated human body model to simulate the human activity within the indoor environments.
- (ii) This study developed an easier 3-D object handling technique to determine the intersection point on the object surfaces, namely surface separation technique.
- (iii) This study introduces Red-Black tree data structure as a new and faster data storage technique for the objects that used for the simulation.
- (iv) In order to optimize the ray tracing time, object address distribution and object searching techniques are used as a new acceleration technique of the proposed model.

5.3 FUTURE WORK

The proposed ray tracing model presented in this dissertation is mainly developed for the populated indoor environment. For more reliable prediction results, a better human like body model will be developed for the real life simulation. This study investigates

the effect of human motion on indoor wave propagation by using 60 GHz frequency. In future, this study will be of interest to work with the high frequency band, like terahertz (THz) frequency to investigate the influence of human motion on radio wave propagation. Moreover, this idea will be implemented for the Wireless Body Area Network in future.

University of Malaya

REFERENCES

- Algiannakis, C., Robertson, I. and Aghivami, A. H. (1995). A 3D raytracing model for the study of sectorized antenna performance in indoor radio communications systems. in Proc. Sixth IEEE International Symposium on Personal, Indoor and Mobile Radio Communications, vol. 2, pp. 414-418.
- Alvar, N. S., Ghorbani, A. and Amindavar, H. (2008). A novel hybrid approach to raytracing acceleration based on pre-processing and bounding volumes. Progress In Electromagnetics Research, vol. 82, pp. 19-32.
- Anderson, C. R. and Rappaport, T. S. (2004). In-building wideband partition loss measurements at 2.5 and 60 GHz. IEEE Transactions on Wireless Communications, vol. 3, no. 3, pp. 922-928.
- Aparicio, J., Jimé'nez, A., lvarez, F. J. A., Uren~a, J., Marziani, C. D. and Diego, C. (2011). Modeling the Behavior of an Underwater Acoustic Relative Positioning System Based on Complementary Set of Sequences. Sensors, vol. 11, pp. 11188-11205.
- Bensebti, M., McGeehan, J. P. and Beach, M. A. (1991). Indoor multipath radio propagation measurements and characterisation at 60 GHz. 21st European Conference on Microwave, vol. 2, pp. 1217-1222.
- Bird, T. S., Kot, J. S., Nikolic, N., James, G. L. and Barker, S. J. (1994). Millimetre-wave antenna and propagation studies for indoor wireless LANs. Antennas and Propagation Society International Symposium, vol. 1, pp. 336-339.
- Burnside, W. and Burgener, K. (1983). High frequency scattering by a thin lossless dielectric slab. IEEE Transactions on Antennas and Propagation Magazine, vol. 31, no. 1, pp. 104-110.
- Catedra, M. F. (1999). Cell Planning for Wireless Communications Artech House.
- Catedra, M. F., Perez, J., Saez de Adana, F. and Gutierrez, O. (1998). Efficient ray-tracing techniques for three-dimensional analyses of propagation in mobile communications: application to picocell and microcell scenarios. IEEE Antennas and Propagation Magazine, vol. 40, no. 2, pp. 15-28.
- Chahat, N., Zhadobov, M., Le Coq, L., Alekseev, S. I. and Sauleau, R. (2012). Characterization of the interactions between a 60-GHz antenna and the human body in an off-body scenario. IEEE Transactions on Antennas and Propagation, vol. 60, no. 12, pp. 5958-5965.
- Chiya, S. and H., F. (2010). Modified angular Z-Buffer as an acceleration technique for ray tracing. IEEE Transactions on Antennas and Propagation, vol. 58, no. 5.
- Collonge, S., Zaharia, G. and Zein, G. E. (2004). Influence of the human activity on wide-band characteristics of the 60 GHz indoor radio channel. IEEE Transactions on Wireless Communications, vol. 3, no. 6, pp. 2396-2406.

Daniels, R. C. and Heath, R. W. (2007). 60 GHz wireless communications: emerging requirements and design recommendations. *IEEE Vehicular Technology Magazine*, vol. 2, no. 3, pp. 41-50.

Dardari, D., Minelli, L., Tralli, V. and Andrisano, O. (1996). Wideband indoor, communication channels at 60 GHz. *Seventh IEEE International Symposium on Personal, Indoor and Mobile Radio Communications*, vol. 3, pp. 791-794.

Davies, R., Bensebti, M., Beach, M. A. and McGeehan, J. P. (1991). Wireless propagation measurements in indoor multipath environments at 1.7 GHz and 60 GHz for small cell systems. *41st IEEE Vehicular Technology Conference, Gateway to the Future Technology in Motion*, St. Louis, MO, pp. 589-593.

De Adana, F. S., Gutierrez Blanco, O., Diego, I. G., Perez Arriaga, J. and Catedra, M. F. (2000). Propagation model based on ray tracing for the design of personal communication systems in indoor environments. *IEEE Transactions on Vehicular Technology*, vol. 49, no. 6, pp. 2105-2112.

Degli-Esposti, V., Falciasecca, G., Frullone, M. and Riva, G. (1997). Narrowband characterization of 60 GHz radio propagation in indoor environment. *Annals of Telecommunications*, vol. 52, no. 3-4.

Delignon, Y., Clavier, L., Lethuc, V., Garnier, C. and Rachdi, M. (2001). Compound statistical model for 60 GHz channel. *IEEE 54th Vehicular Technology Conference, Atlantic City, NJ*, vol. 3, pp. 1780-1784.

Dersch, U. and Zollinger, E. (1994). Propagation mechanisms in microcell and indoor environments. *IEEE Transactions on Vehicular Technology*, vol. 43, no. 4, pp. 1058-1066.

Dikmen, F., Ergin, A. A., Sevgili, A. L. and Terzi, B. (2010). Implementation of an efficient shooting and bouncing rays scheme. *Microwave and Optical Technology Letters*, vol. 52, pp. 2409-2413.

Diskin, J. and Brennan, C. (2007). Accelerated ray-tracing for indoor ultra-wideband propagation modelling. *IEEE 65th Vehicular Technology Conference, Dublin*, pp. 418-422.

Fernandes, J. J. G., Smulders, P. F. M. and Neves, J. C. (1994). Simulation results on MM-wave indoor radio channel modelling and comparison with measurements. *IEEE Second Symposium on Communications and Vehicular Technology in the Benelux, Louvain la Neuve*, pp. 89-94.

Floyd, B. A., Reynolds, S. K., Pfeiffer, U. R., Zwick, T., Beukema, T. and Gaucher, B. (2005). SiGe bipolar transceiver circuits operating at 60 GHz. *IEEE Journal of Solid-State Circuits*, vol. 40, no. 1, pp. 156-167.

Fluerasu, A. and Letrou, C. (2009). Gaussian beam launching for 3D physical modeling of propagation channels. *Annals of Telecommunications*, vol. 64, pp. 763-776.

Friis, H. T. (1946). A note on a simple transmission formula. *Proc. IRE*, vol. 34, pp. 254.

Garnier, C., Clavier, L., Delignon, Y., Loosvelt, M. and Boulinguez, D. (2002). Multiple access for 60 GHz mobile ad hoc network. IEEE 55th Vehicular Technology Conference, vol. 3, pp. 1517-1521.

Gatland, I. R. (2002). Thin lens ray tracing. American J. Phys., vol. 70, pp. 1184.

Genc, Z., Thillo, W. V., Bourdoux, A. and Onur, E. (2012). 60 GHz PHY performance evaluation with 3D ray tracing under human shadowing. Wireless Communications Letters, IEEE, vol. 1, no. 2, pp. 117-120.

Ghannoum, I., Letrou, C. and Beauquet, G. (2009). A Gaussian beam shooting algorithm for radar propagation simulations. IEEE International Radar Conference - Surveillance for a Safer World, Bordeaux, pp. 1-5.

Gustafson, C. and Tufvesson, F. (2012). Characterization of 60 GHz shadowing by human bodies and simple phantoms. 6th European Conference on Antennas and Propagation (EUCAP), pp. 473-477.

Haibing, Y., Herben, M. H. A. J. and Smulders, P. F. M. (2006). Indoor radio channel fading analysis via deterministic simulations at 60 GHz. 3rd International Symposium on Wireless Communication Systems, pp. 144-148.

Hammoudeh, A. and Haslett, C. (1995). Characterisation and modelling of obstructed line-of-sight millimetre wave mobile radio signals. Ninth International Conference on Antennas and Propagation, vol. 2, pp. 283-287.

Hansen, J. (2002). A novel stochastic millimeter-wave indoor radio channel model. IEEE Journal on Selected Areas in Communications, vol. 20, no. 6, pp. 1240-1246.

Hoppe, R., Wolfle, G. and Landstorfer, F. M. (1999). Measurement of building penetration loss and propagation models for radio transmission into buildings. IEEE VTS 50th Conference on Vehicular Technology, Amsterdam, vol. 4, pp. 2298-2302.

Iskander, M. F. and Yun, Z. (2002). Propagation prediction models for wireless communication systems. IEEE Transactions on Microwave Theory and Techniques, vol. 50, no. 3, pp. 662-673.

Jacob, M., Mbianke, C. and Kurner, T. (2010). A dynamic 60 GHz radio channel model for system level simulations with MAC protocols for IEEE 802.11ad. IEEE 14th International Symposium on Consumer Electronics (ISCE), Braunschweig, pp. 1-5.

Jacob, M., Priebe, S., Kurner, T., Peter, M., Wisotzki, M., Felbecker, R. and Keusgen, W. (2013). Fundamental analyses of 60 GHz human blockage. 7th European Conference on Antennas and Propagation (EuCAP), pp. 117-121.

Jacob, M., Priebe, S., Maltsev, A., Lomayev, A., Erceg, V. and Kurner, T. (2011). A ray tracing based stochastic human blockage model for the IEEE 802.11ad 60 GHz channel model. IEEE 5th European Conference on Antennas and Propagation (EUCAP), Rome, pp. 3084-3088.

Janaswamy, R. (2006). An indoor pathloss model at 60 GHz based on transport theory. IEEE Antennas and Wireless Propagation Letters, vol. 5, no. 1, pp. 58-60.

Jarvelainen, J., Haneda, K., Kyro, M., Kolmonen, V. M., Takada, J. and Hagiwara, H. (2012). 60 GHz radio wave propagation prediction in a hospital environment using an accurate room structural model. *Antennas and Propagation Conference (LAPC)*, pp. 1-4.

Khafaji, A., Saadane, R., El Abbadi, J., and Belkasmi, M. (2008). Ray tracing technique based 60 GHz band propagation modelling and influence of people shadowing. *World Academy of Science Engineering and Technology*, vol. 45.

Kim, B.-C., Park, K. K. and Kim, H.-T. (2009). Efficient RCS prediction method using angular division algorithm. *Journal of Electromagnetic Waves and Application*, vol. 23, no. 1, pp. 65-74.

Kouyoumjian, R. G. and Pathak, P. H. (1974). A uniform geometrical theory of diffraction for an edge in a perfectly conducting surface. *Proceedings of the IEEE*, vol. 62, no. 11, pp. 1448-1461.

Kyro, M., Simola, J., Haneda, K., Ranvier, S., Vainikainen, P. and Takizawa, K. i. (2010). 60 GHz Radio channel measurements and modeling in a shielded room. *IEEE 71st Conference on Vehicular Technology, Taipei*, pp. 1-5.

Langen, B., Lober, G. and Herzig, W. (1994). Reflection and transmission behaviour of building materials at 60 GHz. *5th IEEE International Symposium on Personal, Indoor and Mobile Radio Communications The Hague*, vol. 2, pp. 505-509.

Lawton, M. C. and McGeehan, J. P. (1994). The application of a deterministic ray launching algorithm for the prediction of radio channel characteristics in small-cell environments. *IEEE Transactions on Vehicular Technology*, vol. 43, no. 4, pp. 955-969.

Letrou, C. (2007). A Gaussian beam shooting scheme for fast multidimensional physical simulation of propagation channels in wireless communication systems. *International Conference on Electromagnetics in Advanced Applications (ICEAA)*, Torino, Italy, pp. 33-36.

Liang, C., Liu, Z. and Di, H. (2008). Study on the blockage of electromagnetic rays analytically. *Progress In Electromagnetics Research B*, vol. 1, pp. 253-268.

Liang, G. and Bertoni, H. L. (1998). A new approach to 3-D ray tracing for propagation prediction in cities. *IEEE Transactions on Antennas and Propagation*, vol. 46, no. 6, pp. 853-863.

Liihteenmiiki, J. and Karttaavi, T. (1996). Measurement of dielectric parameters of wall materials at 60GHz band. *Electronic Letters*, vol. 32, no. 16, pp. 1442-1444.

Lim, C.-P., Lee, M., Burkholder, R. J., Volakis, J. L. and Marhefka, R. J. (2007). 60 GHz indoor propagation studies for wireless communications based on a ray-tracing method. *EURASIP Journal on Wireless Communications and Networking*, vol. 2007, no. 073928.

Lim, C. -P., Burkholder, R. J., Volakis, J. L. and Marhefka, R. J. (2006). Propagation modeling of indoor wireless communications at 60 GHz. *IEEE Antennas and Propagation Society International Symposium*, pp. 2149-2152.

- Lostanlen, Y., Corre, Y., Louet, Y., Le Helloco, Y., Collonge, S. and El-Zein, G. (2002). Comparison of measurements and simulations in indoor environments for wireless local networks at 60 GHz. *IEEE 55th Vehicular Technology Conference*, vol. 1, pp. 389-393.
- Luebbers, R. (1984). Finite conductivity uniform GTD versus knife edge diffraction in prediction of propagation path loss. *IEEE Transactions on Antennas and Propagation*, vol. 32, no. 1, pp. 70-76.
- Maltsev, A., Maslennikov, R., Sevastyanov, A., Khoryaev, A. and Lomayev, A. (2009). Experimental investigations of 60 GHz WLAN systems in office environment. *IEEE Journal on Selected Areas in Communications*, vol. 27, no. 8, pp. 1488-1499.
- Marinier, P., Delisle, G. Y. and Despins, C. L. (1998). Temporal variations of the indoor wireless millimeter-wave channel. *IEEE Transactions on Antennas and Propagation*, vol. 46, no. 6, pp. 928-934.
- McKown, J. W. and Hamilton, R. L., Jr. (1991). Ray tracing as a design tool for radio networks. *IEEE Network*, vol. 5, no. 6, pp. 27-30.
- Minyoung, P. and Gopalakrishnan, P. (2009). Analysis on spatial reuse and interference in 60-GHz wireless networks. *IEEE Journal on Selected Areas in Communications*, vol. 27, no. 8, pp. 1443-1452.
- Mohtashami, V. and Shishegar, A. A. (2010). Accuracy and computational efficiency improvement of ray tracing using line search theory. *IET Microwaves, Antennas & Propagation*, vol. 4, no. 9, pp. 1290-1299.
- Mohtashami, V. and Shishegar, A. A. (2010). Efficient shooting and bouncing ray tracing using decomposition of wavefronts. *IET Microwaves, Antennas & Propagation*, vol. 4, no. 10, pp. 1567-1574.
- Mohtashami, V. and Shishegar, A. A. (2012). Modified wavefront decomposition method for fast and accurate ray-tracing simulation. *IET Microwaves, Antennas & Propagation*, vol. 6, no. 3, pp. 295-304.
- Moraitis, N. and Constantinou, P. (2002). Indoor channel modeling at 60 GHz for wireless LAN applications. *IEEE International Symposium on Personal, Indoor and Mobile Radio Communication*, vol. 3, pp. 1203-1207.
- Moraitis, N. and Constantinou, P. (2004). Indoor channel measurements and characterization at 60 GHz for wireless local area network applications. *IEEE Transactions on Antennas and Propagation*, vol. 52, no. 12, pp. 3180-3189.
- Morgadinho, S., Caldeirinha, R. F. S., Al-Nuaimi, M. O., Cuinas, I., Sanchez, M. G., Fernandes, T. R. and Richter, J. (2012). Time-variant radio channel characterization and modelling of vegetation media at millimeter-wave frequency. *IEEE Transactions on Antennas and Propagation*, vol. 60, no. 3, pp. 1557-1568.

- Nobles, P. and Halsall, F. (1999). Indoor propagation at 17 GHz and 60 GHz-measurements and modelling. IEE National Conference on Antennas and Propagation, pp. 93-96.
- O'Rourke, J. (1993). Computational Geometry in C. Cambridge, U. K.: Cambridge Univ. Press.
- Oliver, A. D. (1989). Millimeter wave systems – past, present and future. IEE Proceedings, vol. 136, no. 1, pp. 35-52.
- Pena, D., Feick, R., Hristov, H. D. and Grote, W. (2003). Measurement and modeling of propagation losses in brick and concrete walls for the 900-MHz band. IEEE Transactions on Antennas and Propagation, vol. 51, no. 1, pp. 31-39.
- Qiu, R. C., Huaping, L. and Xuemin, S. (2005). Ultra-wideband for multiple access communications. IEEE Communications Magazine, vol. 43, no. 2, pp. 80-87.
- Raida, Z., Lukes, Z. and Lacik, J. (2008). On using Ray-Launching method for modeling rotational spectrometer. Radioengineering, vol. 17, no. 2, pp. 98-107.
- Ramo, S. (1997). Fields and waves in communication electronics. New York: John Wiley.
- Rao, T. R., Murugesan, D., Ramesh, S. and Labay, V. A. (2011). Radio channel characteristics in an indoor corridor environment at 60 GHz for wireless networks. IEEE 5th International Conference on Advanced Networks and Telecommunication Systems (ANTS), Bangalore, pp. 1-5.
- Reza, A. W., Dimiyati, K., Noordin, K. A., Kausar, A. S. M. Z. and Sarker, M. S. (2012). A comprehensive study of optimization algorithm for wireless coverage in indoor area. Optimization Letters. doi:10.1007/s11590-012-0543-z
- Rougerona, G., Gaudairea, F.-c., Gabilleta, Y. and Bouatouchb, K. (2002). Simulation of the indoor propagation of a 60GHz electromagnetic wave with a time-dependent radiosity algorithm. Computers & Graphics, vol. 26, pp. 125-141.
- Saeidi, C. and Hodjatkashani, F. (2010). Modified angular Z-buffer as an acceleration technique for ray tracing. IEEE Transactions on Antennas and Propagation, vol. 58, no. 5, pp. 1822-1825.
- Saeidi, C., Hodjatkashani, F. and Fard, A. (2009). New tube-based shooting and bouncing ray tracing method. International Conference on Advanced Technologies for Communications, pp. 269-273.
- Saeidi, C., Kamyab, M. and Fard, A. (2006). Fast ray tracing propagation prediction model for indoor environments. 7th International Symposium on Antennas, Propagation & EM Theory, pp. 1-4.
- Sandor, Z., Nagy, L., Szabo, Z. and Csaba, T. (1997). 3D ray launching and moment method for indoor radio propagation purposes. The 8th IEEE International Symposium on Personal, Indoor and Mobile Radio Communications, vol. 1, pp. 130-134.

Sato, R. and Shirai, H. (2008). Simplified ray-launching analysis for indoor propagation including multiple reflection effect inside walls. IEEE Antennas and Propagation Society International Symposium, pp. 1-4.

Sato, R. and Shirai, H. (2009). Efficient ray-launching analysis for indoor propagation including multiple reflection effect inside walls. International Conference on Electromagnetics in Advanced Applications, pp. 756-759.

Seidel, S. Y. and Rappaport, T. S. (1994). Site-specific propagation prediction for wireless in-building personal communication system design. IEEE Transactions on Vehicular Technology, vol. 43, no. 4, pp. 879-891.

Shen, X., Guizani, M., Chen, H. H., Qiu, R. C., Molisch, A. F. and Milstein, L. B. (2006). Guest editorial ultra-wideband wireless communications: Theory and applications. IEEE Journal on Selected Areas in Communications, vol. 24, no. 4, pp. 713-716.

Siamarou, A. G. (2003). Broadband wireless local area networks at millimeter waves around 60 GHz. IEEE Antennas and Propagation Magazine, vol. 45, no. 1, pp. 177-181.

Siamarou, A. G. (2003). Wideband propagation measurements and channel implications for indoor broadband wireless local area networks at the 60 GHz band. Wireless Personal Communications, vol. 27, pp. 89-98.

Smith, C. J. (1963). A Degree Physics, Part III, Optics. London: Edward Arnold Publishers.

Smulders, P. and Correia, L. (1997). Characterisation of propagation in 60 GHz radio channels. Electronic and Communication Engineering Journal, vol. 9, no. 2, pp. 73-80.

Smulders, P. F. M. (2009). Statistical characterization of 60-GHz indoor radio channels. IEEE Transactions on Antennas and Propagation, vol. 57, no. 10.

Tahri, R., Letrou, C. and Hanna, V. F. (2002). A beam launching method for propagation modeling in multipath contexts. Microwave and Optical Technology Letters, vol. 35, no. 1, pp. 6-10.

Talbi, L. (2001). Human disturbance of indoor EHF wireless channel. Electronic Letters, vol. 37, pp. 1361-1363.

Tam, W. K. and Tran, V. N. (1995). Propagation modelling for indoor wireless communication. Electronics & Communication Engineering Journal, vol. 7, no. 5, pp. 221-228.

Tao, Y. B., Lin, H. and Bao, H. J. (2008). Kd-tree based fast ray tracing for RCS prediction. Progress In Electromagnetics Research, vol. 81, pp. 329-341.

Thomas, H., Cormen, C., Ronald, E. L. and Stein, L. R. C. (2001). Introduction to Algorithms. Massachusetts London, England: The MIT Press Cambridge.

Tsingos, N., Funkhouser, T., Ngan, A. and Carlbom, I. (2001). Modelling acoustics in virtual environments using the uniform theory of diffraction. Proceedings of the 28th

annual conference on Computer graphics and interactive techniques, Los Angeles, CA, USA, pp. 545-552.

Wales, S. W. (1990). Channel modelling and equalisation techniques for broadband mobile communications at 60 GHz. in Proc. IEE Colloquium on Methods of Combating Multipaths, pp. 7/1-7/8.

Wales, S. W., Rickard, D. C., Beach, M. A. and Davies, R. (1991). Measurement and modelling of short range broadband millimetric mobile communication channels. IEE Colloquium on Radiocommunications in the Range 30-60 GHz, pp. 12/1-12/6.

Wang, X. B., Zhou, X. Y., Cui, T. J., Tao, Y. B. and Lin, H. (2008). High-resolution inverse synthetic aperture radar imaging based on the shooting and bouncing ray method. Global Symposium on Millimeter Waves, pp. 1-3.

Williamson, M. R., Athanasiadou, G. E. and Nix, A. R. (1997). Investigating the effects of antenna directivity on wireless indoor communication at 60 GHz. The 8th IEEE International Symposium on Personal, Indoor and Mobile Radio Communications, vol. 2, pp. 635-639.

Win, M. Z. and Scholtz, R. A. (2000). Ultra-wide bandwidth time-hopping spread-spectrum impulse radio for wireless multiple-access communications. IEEE Transactions on Communications, vol. 48, no. 4, pp. 679-689.

Xu, H., Kukshya, V. and Rappaport, T. (2002). Spatial and temporal characterization of 60 GHz Indoor channels. IEEE Journal on selected areas in communications, vol. 20 no. 3, pp. 620-630.

Yang, H., Smulders, P. F. M. and Herben, M. H. A. J. (2005). Indoor channel measurements and analysis in the frequency bands 2 GHz and 60 GHz. IEEE 16th International Symposium on Personal, Indoor and Mobile Radio Communications, 11-14 Sept., Berlin, vol. 1, pp. 579 - 583.

Yongming, Huang, Alain, C., Larbi, T. and Tayeb, A. D. (2006). Effect of human body upon line-of-sight indoor radio propagation. Canadian Conference on Electrical and Computer Engineering, pp. 1775-1778.

Young-Keun, Y., Myoung-won, J. and JongHo, K. (2011). Analysis and comparison on roughness at millimetre wave. 13th International Conference on Advanced Communication Technology (ICACT), pp. 1316-1319.

Youssef, A., Mon, J. P., Meynard, O., Nkwawo, H., Meyer, S. and Leost, J. C. (1994). Indoor wireless data systems channel at 60 GHz modeling by a ray-tracing method. IEEE 44th Vehicular Technology Conference, vol. 2, pp. 914-918.

Zhihua, L., Bessis, N., Roche, G. d. l., Kuonen, P., Zhang, J. and Clapworthy, G. (2009). A new approach to solve angular dispersion of discrete ray launching for urban scenarios. Antennas & Propagation Conference, Loughborough, pp. 133-136.

Zhong, F. (2008). Wireless networking with directional antennas for 60 GHz systems. 14th European Conference on Wireless, 22-25 June, Prague, pp. 1-7.

Zwick, T., Beukema, T. J. and Haewoon, N. (2005). Wideband channel sounder with measurements and model for the 60 GHz indoor radio channel. IEEE Transactions on Vehicular Technology, vol. 54, no. 4, pp. 1266-1277.

University of Malaya

LIST OF ISI PUBLICATIONS

- [1] **M. J. Islam**, A. W. Reza, K. A. Noordin, A. S. M. Z. Kausar, and R. Harikrishnan, "Efficient and Accurate Ray Tracing Method for Indoor Radio Wave Propagation Prediction in Presence of Human Body Movement", *Journal of Electromagnetic Waves and Applications*, Vol. 27, No. 12, 1566-1586, 2013.
- [2] **M. J. Islam**, A. W. Reza, K. A. Noordin, A. S. M. Z. Kausar, and R. Harikrishnan, "Red-black Tree Based Fast and Accurate Ray Tracing for Indoor Radio Wave Prediction", *Frequenz, Journal of RF-Engineering and Telecommunications*, Vol. 67, No. 9-10, 2013.
- [3] **M. J. Islam**, A. W. Reza, K. A. Noordin, K. Dimiyati, and A. S. M. Z. Kausar. "An Accelerated and Accurate Three-Dimensional Ray Tracing Using Red-Black Tree with Facet Mining and Object Bouncing Techniques", *Turkish Journal of Electrical Engineering & Computer Sciences*, DOI: 10.3906/elk-1212-98.
- [4] **M. J. Islam**, A. S. M. Z. Kausar, A. W. Reza, and K. A. Noordin. "Investigation of the Effect of Human Motion on Indoor Radio Signal Propagation," In: *2nd International Conference on Power and VLSI Engineering (ICPVE'2013)*, May 6-7, 2013, Kuala Lumpur, Malaysia, pp. 31-35.